# Petrologic Characterization of Pelitic Schists in the Western Metamorphic Belt, Coast Plutonic-Metamorphic Complex, Near Juneau, Southeastern Alaska

*By* Glen R. Himmelberg, David A. Brew, *and* Arthur B. Ford

U.S. GEOLOGICAL SURVEY BULLETIN 2074


UNITED STATES GOVERNMENT PRINTING OFFICE, WASHINGTON : 1994

# U.S. DEPARTMENT OF THE INTERIOR

## BRUCE BABBITT, Secretary

## U.S. GEOLOGICAL SURVEY

### Robert M. Hirsch, Acting Director

For sale by
USGS Map Distribution
Box 25286 MS306
Denver Federal Center
Denver, CO 80225



Text and illustrations edited by James W. Hendley II

**Library of Congress Cataloging-in-Publication Data**

Himmelberg, Glen R.
Petrologic characterization of pelitic schists in the western metamorphic belt, coast plutonic-metamorphic complex, near Juneau, southeastern Alaska / by Glen R. Himmelberg, David A. Brew, and Arthur B. Ford.
p. cm. — (U.S. Geological Survey bulletin ; 2074)
Includes bibliographical references.
1. Schists—Alaska—Juneau Region. 2. Geology—Alaska—Juneau Region. I. Brew, David A. II. Ford, Arthur B. (Arthur Barnes), 1932– III. Title. IV. Series.
QE75.B9 no. 2074
[QE475.S3]
557.3 s—dc20 94-293
[552'.4] CIP

# CONTENTS



## FIGURES



## TABLES

# Petrologic Characterization of Pelitic Schists in the Western Metamorphic Belt, Coast Plutonic-Metamorphic Complex, Near Juneau, Southeastern Alaska

*By* Glen R. Himmelberg, David A. Brew *and* Arthur B. Ford

## ABSTRACT

The metamorphic rocks exposed near Juneau, Alaska, are part of the western metamorphic belt of the Coast plutonic-metamorphic complex of western Canada and southeastern Alaska. This belt underwent a complex history of deformation, metamorphism, and plutonism that ranges in age from about 120 to 50 Ma as a result of tectonic overlap and (or) compressional thickening of crustal rocks during collision of the Alexander and Stikinia terranes. Most of the schists near Juneau were metamorphosed during the M5 metamorphic event about 70 m.y. ago and are part of a belt of schists of similar metamorphic age that extends for at least 400 km to the southeast. Distribution of pelitic mineral isograds, systematic changes in mineral assemblages, and silicate geothermometry of the Juneau schists indicate an inverted metamorphic gradient over a distance of about 5 km. Changes in mineral assemblages across isograds separating the metamorphic zones are in general agreement with discontinuous reactions in the ideal $SiO_2$-$Al_2O_3$-$K_2O$-FeO-MgO-$H_2O$ system. Biotite and staurolite in low variance assemblages show changes in Mg/(Mg+Fe) ratios with metamorphic grade that are generally consistent with predicted changes in the ideal system, although exceptions exist. The observed metamorphic mineral assemblages and previously determined peak temperatures and pressures (530°C for the garnet zone to about 705°C for the upper kyanite-biotite zone, and 9 to 11 kbar) are consistent with recently published petrogenetic grids for pelitic rocks. Maximum mole fraction of $H_2O$ as constrained by distribution of species in the C-O-H system for graphitic schists ranges from about 0.93 for the garnet zone to about 0.90 for the upper kyanite-biotite zone. Metamorphic mineral growth was synchronous with the third of four recognized folding events.

Manuscript approved for publication, October 14, 1993.

## INTRODUCTION

The metamorphic rocks exposed near Juneau, Alaska are part of the western metamorphic belt of the informally named Coast plutonic-metamorphic complex (Brew and Ford, 1984) of western Canada and southeastern Alaska (fig. 1). The western metamorphic belt and associated plutons developed as a result of tectonic overlap and (or) compressional thickening of crustal rocks during the collision of two large allochthonous terranes—the Alexander terrane on the west and the Stikinia terrane to the east (Monger and others, 1982; Brew and Ford, 1983). The western metamorphic belt is one of the major metamorphic features of southeastern Alaska (Brew and others, 1992).

The western metamorphic belt ranges from a few kilometers to several tens of kilometers wide and is characterized in general by Barrovian metamorphism. The metamorphic grade increases to the northeast, with the highest grade adjacent to the plutonic part of the Coast plutonic-metamorphic complex. At the latitude of Juneau the western metamorphic belt is about 30 km wide. The mineral isograds, systematic changes in mineral assemblages, and structural relations indicate an inverted metamorphic gradient along the easternmost part of the belt, where the metamorphic grade goes abruptly from pumpellyite-actinolite facies to kyanite- and sillimanite-bearing amphibolite facies in less than 5 km across strike.

The development of the inverted metamorphic sequence and the geothermometry and geobarometry associated with its formation was recently discussed by Himmelberg and others (1991). This report extends that work to include more detailed data on mineral assemblages, metamorphic reactions, structural relations, age constraints, and mineral chemistry that were not included in the earlier paper. These data and discussions provide a more complete characterization of the western metamorphic belt in the Juneau area and, along with the earlier paper, will serve as a foundation to continually evaluate the evolution of western metamorphic belt as other data are obtained.

## ACKNOWLEDGMENTS

We thank J.H. Dover and R.W. Tabor for helpful reviews of this manuscript and Dan Kremser for his help in using the electron microprobe at Washington University.

## WESTERN METAMORPHIC BELT

The western metamorphic belt underwent a complex history of deformation, metamorphism, and plutonism that ranges in age from about 120 Ma to about 50 Ma (Crawford and others, 1987; Brew and others, 1989). The belt varies along and across strike in protolith and metamorphic grade. The belt also varies along strike in the nature of its contact with the dominant granitic part of the Coast plutonic-metamorphic complex. Although we cannot discuss the topic fully here, our analysis of the regional variations indicates that the western metamorphic belt near Juneau contains all of the belt's subparts, whereas most other areas do not. The Juneau area is, therefore, considered to be representative of the whole regional belt.

The protoliths for the western metamorphic belt were mainly the heterogeneous rocks of the Alexander terrane of Permian and Triassic age and the flysch and volcanic rocks of the Gravina overlap assemblage (Berg and others, 1972) of Late Jurassic through early Late Cretaceous age. In the Juneau area, intermixed pelitic and semipelitic metasedimentary rocks and mafic metavolcanic and intrusive rocks are dominant. Impure calcareous metasedimentary rocks, quartzite, and quartz diorite and granodioritic orthogneiss are also present.

The regional history of the Coast plutonic-metamorphic complex was comprehensively summarized by Brew

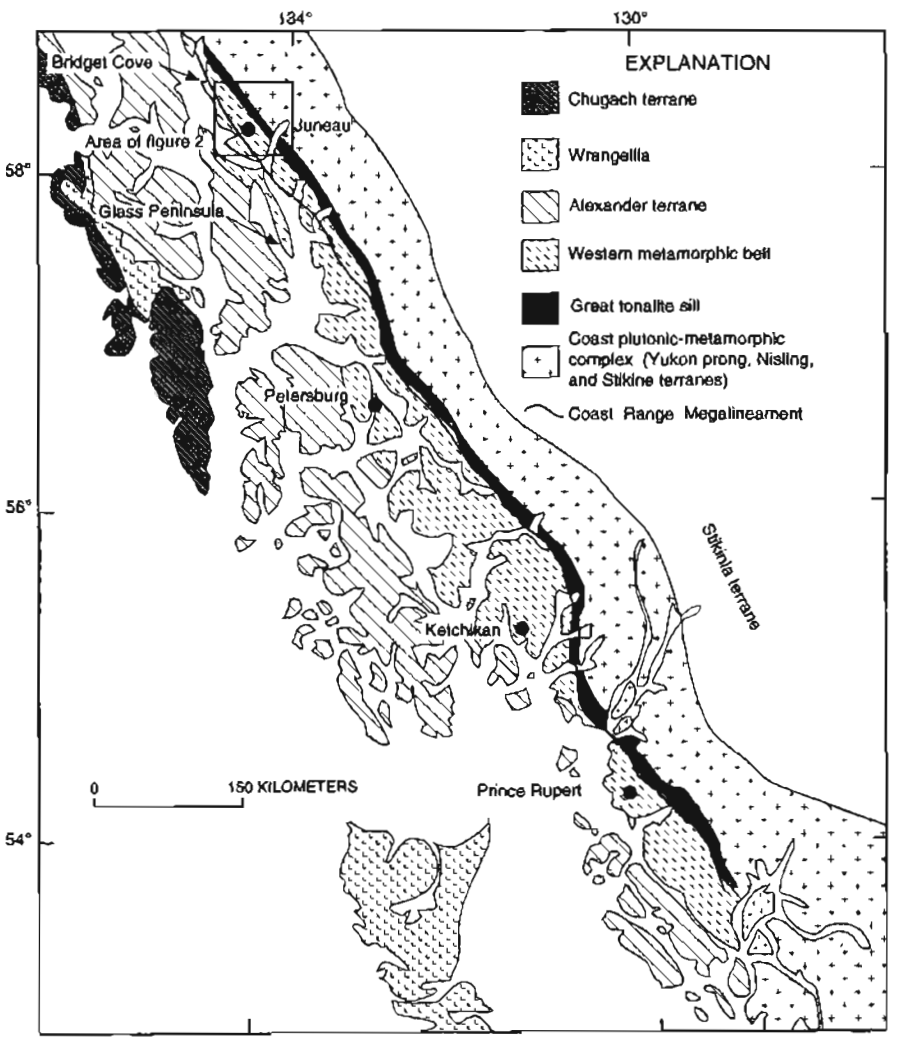


**Figure 1.** Index map showing Coast plutonic-metamorphic complex of Brew and Ford (1984), western metamorphic belt, and terrane boundaries, southeastern Alaska (modified from Himmelberg and others, 1991).

**Table 1.** Approximate time relations of plutonic, deformational, and metamorphic events in the western metamorphic belt of the Coast plutonic-metamorphic complex (from Brew and others, 1989).

| | Time (Ma) | | | | | | | |
|---|---|---|---|---|---|---|---|---|
| Type | 120 | 110 | 100 | 90 | 80 | 70 | 60 | 50 |
| Plutonic events | | P1 | P2 | P3 | | P4 | P5 | P6 |
| Deformational events. | D1 | | | D2 | | D3<br>D4<br>D5 | D4?<br>D5? | D6? |
| Metamorphic events. | M1 | M2 | M3 | M4<br>M4′ | | M5 | M5? | M6 |

and others (1989) in terms of discrete deformational, metamorphic, and plutonic events (table 1). The earliest documented metamorphic event, M1, occurred prior to 110 Ma and was dynamothermal; the extent of the area affected and the metamorphic grade (probably up to greenschist facies) are not well known owing to later metamorphic overprinting. In the Juneau area, metabasites along the westernmost part of the belt contain M1 mineral assemblages characteristic of the pumpellyite-actinolite facies (Himmelberg and others, in press). Metamorphic events M2 (110 Ma), M3 (100 Ma), and M6 (50 Ma) were mostly thermal events that developed aureoles around discrete plutons emplaced during regionally extensive magmatic episodes.

The M4 and M4′ metamorphic events were in response to intrusion of widely separated distinctive granitic to dioritic plutons that range in age from 85 to 101 Ma, and average 95 Ma (P3 plutonic event, Brew and others, 1989). Most of these plutons were statically emplaced and have narrow thermal aureoles (M4), but the larger bodies are syntectonic and are surrounded by closely spaced Barrovian isograds (M4′). These plutons and associated metamorphic rocks occur along much of the length of the western metamorphic belt but are best developed south of the Juneau area. Near Juneau west of the Coast Range megalineament (Brew and Ford, 1978), the 95-Ma plutons and associated aureoles occur in the subgreenschist-facies metamorphic rocks. East of the megalineament, M4 mineral assemblages have been overprinted by the later M5 dynamothermal metamorphism. The Mount Juneau pluton (fig. 2) may belong to the P3 event (Ford and Brew, 1977b); however, there are no vestiges of what would be M4 or M4′ metamorphism associated with this pluton.

The M5 metamorphic event was also dynamothermal and produced a belt of metamorphic rocks that is up to 10 km or more wide and is well preserved for the northern 400 km of the 700-km-long belt. The M5 metamorphism was accompanied and followed by intrusion of tonalite to diorite plutons (P4 plutonic event, Brew and others, 1989) that make up the large composite sill, referred to most recently by Brew (1988) as the great tonalite sill, which extends along the eastern side of the western metamorphic belt along its entire length (fig. 1). The age of plutons in the great tonalite sill range from about 70 Ma to 55 Ma and average about 65 Ma (Brew and others, 1989). Final emplacement of the great tonalite sill plutons caused local re-equilibration and recrystallization of adjacent schists (M5′ metamorphic event, Himmelberg and others, 1991). On the basis of isotopic ages of plutons and geologic relations, Brew and others (1989) interpreted the age of the M5 and M5′ metamorphism to be between about 70 Ma and 65 Ma (see discussion below). The M5 metamorphism, which is the focus of this paper, produced an inverted metamorphic sequence that dips to the northeast.

Brew and Morrell (1983), Brew (1988), and Brew and others (1989) discussed younger plutonic and associated thermal metamorphic events to the east and west of the western metamorphic belt.

Brew and others (1989) recognized six deformational events in the western metamorphic belt. D1 and D3 were regional folding events that produced southwest vergent folds that plunge northwest and southeast. The D2 and D4 deformations were fold events localized about the 95-Ma plutons and great tonalite sill, respectively. Subsequent deformation produced a persistent mylonite zone (D5 deformation event) that commonly forms the southwest contact of the great tonalite sill. The M5 metamorphism in the Juneau area and elsewhere occurred during the D3 deformation event.

Along its entire length, the western metamorphic belt is divided longitudinally by the prominent Coast Range megalineament (fig. 1) (Brew and Ford, 1978). The megalineament is a locally ductile fault zone (D6 deformation event, Brew and others, 1989) that typically is located near the western edge of the high-grade part of the metamorphic belt. At Juneau the megalineament is the Gastineau Channel fault (fig. 2) along which the M1 metamorphic rocks are structurally juxtaposed against the M5 inverted metamorphic sequence (Himmelberg and others, in press).

Throughout the length of the western metamorphic belt the metamorphic grade increases to the northeast. Disregarding M4 aureoles around 95-Ma plutons, the westernmost part of the belt at any latitude is generally of greenschist or subgreenschist facies; to the east, either at the Coast Range megalineament or several kilometers to the west of it, the metamorphic grade increases abruptly toward the great tonalite sill. To the east of the sill, the metamorphic grade remains high up to where the belt is cut off entirely by granitic rocks of the central granitic belt of the Coast plutonic-metamorphic complex (Brew and Ford, 1984).

Few systematic variations in metamorphic grade have been identified along the strike of the western metamorphic belt in either the low-grade westernmost part or in

the high-grade part east of the great tonalite sill. In the central part of the belt, however, where the grade increases abruptly toward the great tonalite sill, there are differences along strike in the highest grades preserved (Crawford and others, 1987; Stowell, 1989; Himmelberg and others, 1991; McClelland and others, 1991). Some differences may be due, in part, to variations in the original metamorphic conditions, but most are interpreted to be due to the effects of the M5′ thermal metamorphism and to mylonitic deformation (D5) along the footwall of the great tonalite sill. D5 deformation occurred during and after emplacement of the sill, and where it was greatest, as at Berners Bay north of Juneau and along Work Channel near Prince Rupert, British Columbia, all of the record of M5 metamorphism has been destroyed and only the record of the older M1, M4, and M4′ metamorphism is preserved; however, vestiges of the M5′ event are preserved adjacent to the mylonitic footwall of the sill. Where the mylonitic deformation has been the least, as near Wrangell, Alaska (Brew and others, 1984), and Juneau, all of the M5 and M5′ record is preserved. Between these two situations a regular progression in metamorphic grade is observed toward the sill, although isograds may be truncated by the sill (Ford and Brew, 1977b).

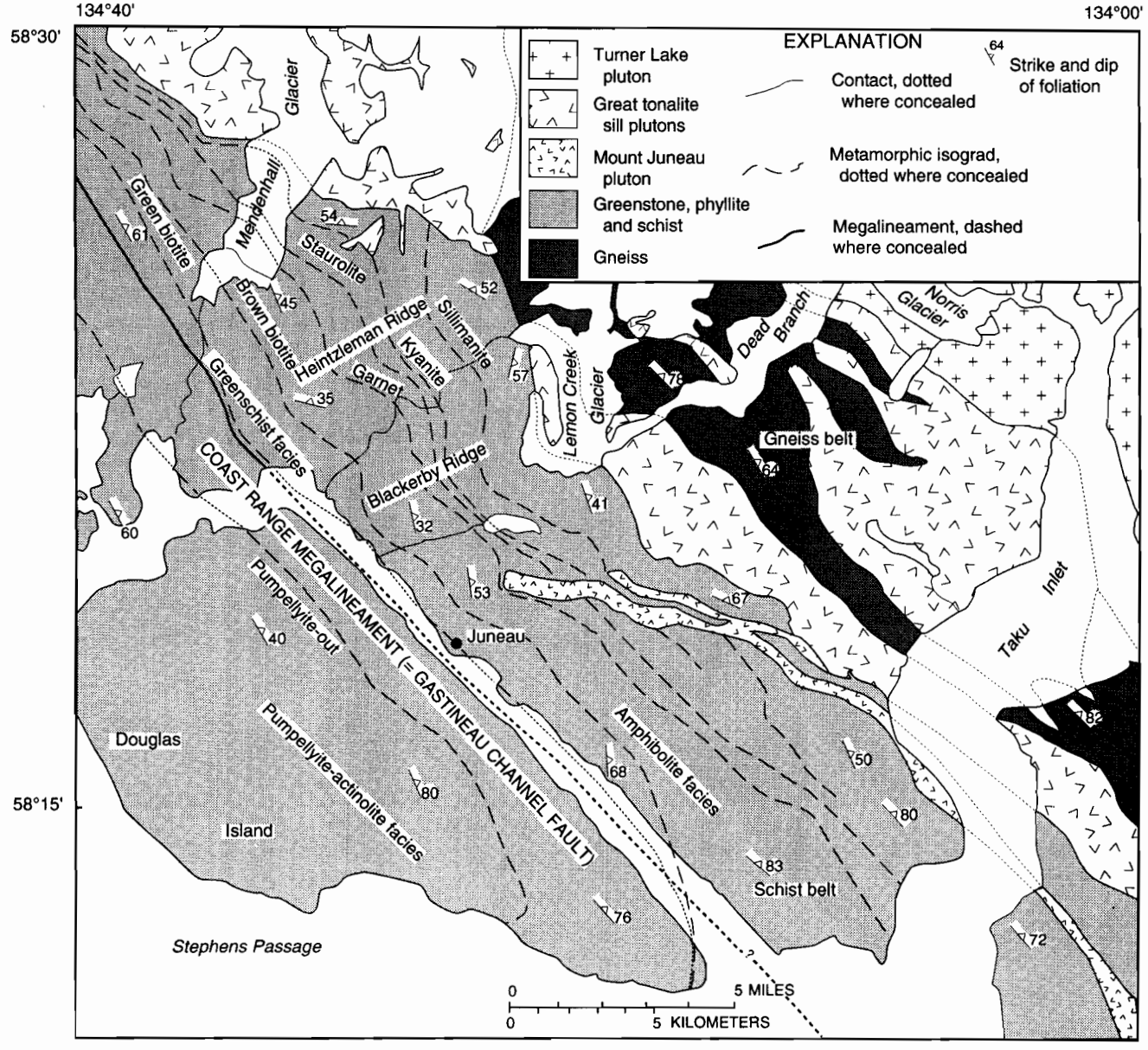


**Figure 2.** Map of Juneau area (parts of the Juneau A1, A2, B1, and B2 quadrangles) showing distribution of metamorphic facies and location of isograds (modified from Ford and Brew, 1973, 1977a; Brew and Ford, 1977; Himmelberg and others, 1991).

## STRUCTURAL RELATIONS

Four phases of deformation have been recognized in the metamorphic rocks of the Juneau area[1]. The oldest phase produced the major schistosity ($S_1$), which is subparallel to compositional layering. The age of this earliest deformation is uncertain; however, on the basis of the timing of porphyroblast growth described below, it predates the M5 metamorphism, and we tentatively equate it to the D1 deformation event of Brew and others (1989), although a D2 age cannot be ruled out. The second phase of deformation recognized in the Juneau area is D3 of Brew and others (1989). The D3 event folded the $S_1$ schistosity about gently plunging (10° to 20°) northwest-trending axes. $F_3$ axial planes are generally steep (55° to 75°) and development of an $S_3$ axial plane foliation is variable. In the field the $S_3$ foliation is generally defined by aligned biotite porphyroblasts and (or ) crenulation of $S_1$. In thin section $S_3$ shows all stages of progressive development (Bell and Rubenach, 1983) from the open crenulation of $S_1$, through crenulation cleavage, to penetrative $S_3$ schistosity. On the limbs of folds, $S_1$ and $S_3$ are subparallel and not readily distinguished. Except in fold hinges, the $S_1$-$S_3$ foliation and compositional layering strikes northwest and dips 25° to 75° to the northeast. Observed amplitudes of $F_3$ folds range from a few centimeters to several tens of meters, and wavelengths range from a few centimeters to many tens of meters. No large-scale structures or minor folds associated with the D1 deformation event have been clearly identified, although there is some suggestion that D1 and D3 may be nearly coaxial.

M5 metamorphism occurred during the D3 deformation event. Inclusion trails in porphyroblasts, particularly biotite and garnet, record the stages of development of $S_3$ crenulation foliation, and where $S_1$ foliation in the rock matrix has been completely obliterated by $S_3$, the porphyroblasts preserve the only evidence of the early $S_1$ foliation (Himmelberg and others, 1984a; Bauer and others, 1988). Similarly, where the late-stage shearing has obliterated evidence for $S_3$ foliation in the matrix of some of the rocks, the porphyroblasts preserve the only evidence for both $S_1$ and $S_3$ foliations (Bauer and others, 1988). The age of the D1 deformation event is unknown but pre-dates the M5 metamorphism.

Evidence for the third phase of deformation in the Juneau area, equivalent to the D4 event of Brew and others (1989), is restricted to the footwall contact of the great tonalite sill where $F_3$ folds are folded about steep axes, which are parallel to hornblende lineations in the sill. Axial planes of these folds parallel the dominant foliation in the metamorphic rocks and sill plutons. The fourth phase of deformation is a shearing event, which is evident from biotite fish and shear bands in the metamorphic rocks (Bauer and others, 1988; Hooper and others, 1990). We tentatively relate this shearing event to uplift associated with the final emplacement of the great tonalite sill and perhaps to early phases of movement on the Coast Range megalineament (D6).

The plutons of the great tonalite sill contain a foliation that is parallel to the $S_3$=$S_1$ foliation in the adjacent metamorphic rocks to the west. The dip of the foliation in the plutons ranges from 45° to 75° to the northeast; three-point dip determinations from individual plutons range from 26° to 60° and average 46°.

## AGE RELATIONS

The timing of deformational, metamorphic, and plutonic events in the western metamorphic belt near Juneau is constrained by fossil data and by K-Ar and U-Pb isotopic-age data from plutons. These data provide limits within which geologic relations are used to interpret the sequence of events.

The maximum age for all events near Juneau is provided by Cretaceous fossils from deformed and low-grade metamorphosed rocks. Three collections (D.L. Jones, written commun., 1969; J.A. Wolfe, oral commun., 1989), two from flyschoid clastic rocks west of the Coast Range megalineament and one from lithologically similar rocks east of it, indicate that rocks as young as Albian (late Early Cretaceous, 113 to 97.5 Ma, Geological Society of America, 1984) and possibly Cenomanian (early Late Cretaceous, 97.5 to 91 Ma, Geological Society of America, 1984) or younger are involved in the earliest deformation (D1).

Isotopic ages have been obtained from plutons representing the five plutonic events that occurred near Juneau. An unpublished U-Pb age determination on zircons from the Jualin pluton in the northern part of the Juneau area indicates that it is about 104 Ma (G.R. Tilton, written commun., 1985), which represents the P2 intrusive event of Brew and others (1989). The age of the P3 intrusive event of Brew and others (1989) in the Juneau area is constrained to about 94 Ma by unpublished U-Pb age determinations on zircons (G.R. Tilton, written commun., 1985; Brew and others, 1992) from the Butler Peak stock on the west side of the Coast Range megalineament and by a confirming K-Ar age determination on hornblende from a compositionally similar pluton on northeastern Admiralty Island (N. Shew, written commun., 1987). J.L. Wooden (written commun., 1988) reported a U-Pb age of

[1]Deformation and metamorphic events in the Juneau area are correlated where possible with the regional events recognized by Brew and others (1989) (table 1). To be consistent with their report, we use their notation and numbering system for the different events.

about 84 Ma and Gehrels and others (1991) reported a U-Pb age of about 72 Ma on zircons from the Mount Juneau pluton. The Mount Juneau pluton underwent deformation and metamorphism during the D3-M5 event (Ford and Brew, 1977b); the M5 isograd surfaces cut the pluton at a high angle, and there is mineralogic evidence of progressive metamorphic changes in the pluton from west to east. K-Ar determinations on coexisting biotite and hornblende from the Mount Juneau pluton yielded discordant ages of about 54 Ma and 66 Ma, respectively (J.G. Smith, written commun., 1974), which are interpreted to be the result of involvement in the later M5 metamorphism and proximity to the great tonalite sill.

U-Pb age determinations on zircons from the Carlson Creek pluton, which is part of the great tonalite sill, indicate that its age is about 67 Ma (Gehrels and others, 1984, 1991). U-Pb ages on zircons from the Mendenhall pluton, which also is part of the great tonalite sill, are about 61.5 Ma (Gehrels and others, 1991). Several K-Ar age determinations on coexisting biotite and hornblende from the Mendenhall pluton yield ages of about 55 Ma (F.J. Wilson, written commun., 1985; F.H. Wilson and N. Shew, written communs., 1986, 1987; N. Shew, written communs., 1987, 1988, 1989). Intrusion of the great tonalite sill plutons represent the P4 plutonic event of Brew and others (1989).

The age of the M5 metamorphism in the Juneau area has not been determined directly by isotopic methods. K-Ar ages ranging from 50.4 to 56.1 Ma were obtained on hornblende and biotite in migmatitic gneisses on Blackerby Ridge and immediately south of Taku Inlet (Forbes and Engels, 1970; F.J. Wilson, written commun., 1985). However the hornblende ages are older than those obtained on coexisting biotite; therefore, these ages probably reflect thermal resetting by the Eocene igneous intrusions (P6).

The age of the M5 metamorphism can be indirectly constrained, however, by the isotopic ages of the great tonalite sill plutons and by geologic relations between the great tonalite sill and the metamorphic rocks. The most important of these relations are as follows:

1. The M5 isograds are in general parallel to the great tonalite sill for long distances, which suggests that the metamorphism was imposed on the region by the regional emplacement of the great tonalite sill. However, the Mount Juneau pluton was affected by the D3-M5 event, which places an upper age limit on the metamorphism, and truncation of the M5 isograds by the great tonalite sill to the north indicates that sill intrusion continued after the isograds were established.

2. The M5 metamorphism accompanied large-scale $F_3$ folding and concomitant development of $S_3$ foliation. On the limbs of folds $S_3$=$S_1$. Foliation within the great tonalite sill is approximately parallel to the $S_3$=$S_1$ foliation in the metamorphic rocks, which suggests that the great tonalite sill was emplaced, at least in part, during the $F_3$ deformation event.

3. Close to the western contact of the sill the $F_3$ folds were locally refolded on steep axes ($F_4$) and hornblende lineations in the sill are parallel to these $F_4$ axes. The development of the $F_4$ structures postdates the development of M5 mineral assemblages, but the absence of new mineral assemblages superimposed on the M5 metamorphism indicates that the pressure-temperature (P-T) conditions at the time of emplacement of the great tonalite sill were not markedly different from those of the M5 metamorphism.

These data suggest that the age of the M5 metamorphism is close to the age of emplacement of the 67±2-Ma and younger great tonalite sill rocks, therefore, Brew and others (1989) tentatively interpreted the M5 metamorphism age to be about 70 Ma.

## METAMORPHIC ZONES AND ISOGRADS

### NATURE AND DEVELOPMENT OF THE INVERTED METAMORPHIC GRADIENT

Forbes (1959) conducted the first systematic study of the distribution of pelitic index minerals along a single transect across the western metamorphic belt near Juneau. In that transect he documented the first appearances of biotite, garnet, staurolite, kyanite, and sillimanite. More extensive mapping by Ford and Brew (1973, 1977a) and Brew and Ford (1977) confirmed and refined Forbes' original interpretation and extended the M5 isograds from Berners Bay on the north to the south side of Taku Inlet. On the basis of more detailed collections, we further revised the isograds in our study area (fig. 2).

The metamorphic zones and isograds define an inverted metamorphic gradient. The isograd surfaces strike northwest and dip to the northeast (fig. 2) and are parallel or subparallel to the dominant metamorphic $S_3$-$S_1$ foliation. Himmelberg and others (1991) reported that the present magnitude of the dip of the isograd surfaces ranges along strike from about 32° to 83° with an average dip of about 62°. However, their attitude has been modified by postmetamorphic Tertiary uplift of the Coast plutonic-metamorphic complex (Crawford and Hollister, 1982; Donelick, 1986; Wood and others, 1987; Zen, 1988; Brew and others, 1989), and a structural evaluation by Himmelberg and others (1991) suggested that the isograd surfaces were originally shallower and ranged in dip from about 42° to 47°.

We also note, however, that the $F_1$ and $F_3$ folds are essentially coaxial, indicating a long history of southwest-vergent folding. Continuation of general large-scale east-over-west movement after the peak of metamorphism could conceivably have rotated and overturned the

isograds from an originally steeper attitude. A continuation of east-over-west movement would also have affected the great tonalite sill plutons. The short time interval available for such a continuation of movement, namely from the 55-Ma emplacement age of the youngest tonalite sill plutons to the 50-Ma emplacement of the voluminous granodiorites of the Coast Mountains, argues against its having had a significant effect.

Pressures and temperatures calculated by Himmelberg and others (1991) indicate that the inverted metamorphic gradient was developed under a pressure of about 9 to 11 kbar with a progressive increase in temperature from about 530°C for the garnet zone to about 705°C for the upper kyanite-biotite zone. Himmelberg and others (1991) interpreted the inverted gradient to have formed during compression of a thickened wedge of relatively wet and cool rocks in response to heat flow associated with the upward movement of the regionally continuous tonalite sill along the east side of the metamorphic belt. Final emplacement of the tonalite sill, during uplift, under pressures of about 5 to 6 kbar caused widespread re-equilibration of garnet rim compositions and growth of chlorite.

## MINERAL ASSEMBLAGES AND MODEL REACTIONS AT ISOGRADS

Mineral assemblages and phase relations in the pelitic rocks of the Juneau area can be analyzed on the $Al_2O_3$-FeO-MgO (AFM) projection of the "ideal" pelitic system $SiO_2$-$Al_2O_3$-$K_2O$-FeO-MgO-$H_2O$ (Thompson, 1957). Listed in table 2 are mineral assemblages that are appropriate to the AFM projection. In addition to the minerals listed, all the assemblages contain quartz and muscovite and may contain plagioclase and the accessory minerals graphite, ilmenite, tourmaline, beryl, sphene, zircon, allanite, and a sulfide mineral. All assemblages also occur in muscovite-deficient quartz-biotite schists, and there are no assemblages in muscovite-deficient rocks that do not occur in muscovite-bearing rocks. Mineral assemblages of all samples studied are listed in table 3. Locations of samples are also given in table 3.

The pelitic mineral assemblages allow us to recognize six distinct metamorphic zones (fig. 2; table 2). The beginning of each zone is marked by the first appearance of the particular index mineral for which it is named. The kyanite-biotite zone is subdivided into upper and lower at the staurolite-out isograd. The phase relations for the garnet through sillimanite zones are shown in figure 3. These phase relations differ slightly from those given by Himmelberg and others (1984b), because a subsequent textural/structural study showed that much of the chlorite previously considered part of the peak metamorphic assemblage is instead of a later generation (Bauer and others, 1988). All five metamorphic zones are well exposed on Heintzleman and Blackerby Ridges near Juneau. To the northwest the higher grade zones are progressively truncated by the great tonalite sill, and to the southeast near Taku Inlet, only the biotite, garnet, and staurolite-biotite zones were recognized. However, H.H. Stowell (oral commun., 1992) recently reported finding kyanite on the northwest shore of Taku Inlet.

The isograds separating the metamorphic zones are marked by the first appearance of the index minerals and can be modeled in the ideal pelitic system by the reactions discussed below (reaction coefficients are not given but can be obtained from Thompson, 1976).

AFM mineral assemblages below and above the garnet isograd (table 2; fig. 3) suggest the model garnet-forming reaction

$$Chl+Ms+Qtz=Grt+Bt+H_2O \qquad (1)$$

This is a divariant continuous reaction; the first appearance of garnet is also dependent on bulk composition and thus may not represent a true isograd.

Mineral assemblages above the garnet-chlorite join have not been observed in the Juneau area. The first appearance of staurolite is at the staurolite-biotite isograd which can be modeled by the discontinuous reaction

$$Chl+Grt+Ms=St+Bt+Qtz+H_2O \qquad (2)$$

The complete reaction assemblage chl-grt-st-bt occurs near the isograd (table 2) in the lowest part of the staurolite-biotite zone. However, chlorite does not persist upward, and most of the staurolite-biotite zone is characterized by the assemblage staurolite-biotite-garnet, which maintains equilibrium by the continuous reaction

$$St+Bt+Qtz=Grt+Ms+H_2O \qquad (3)$$

The stability curve of reaction 3 is nearly flat in P-T space; therefore, as pointed out by Holdaway and others (1982), increasing temperature causes none of the phases to react, grow, or change composition.

In the Juneau area the chlorite-out isograd is nearly coincident with the staurolite-biotite isograd. The AFM topologies of Himmelberg and others (1984b) which showed chlorite persisting into the kyanite-biotite zone, and the chlorite-out isograd as mapped by Ford and Brew (1973, 1977a) and Brew and Ford (1977), as noted above, were based on what now is interpreted as late-generation chlorite.

In other areas of progressive metamorphism (Carmichael, 1970; Guidotti, 1974; Novak and Holdaway, 1981; Holdaway and others, 1982; Klaper and Bucher-Nurminen, 1987) the formation of kyanite (or sillimanite) and the kyanite (or sillimanite) -biotite isograd results from the model discontinuous reaction

$$Chl+St+Ms=Ky+Bt+Qtz+H_2O \qquad (4)$$

**Table 2.** Observed mineral assemblages in the Juneau area appropriate to Thompson's (1957) $Al_2O_3$-FeO-MgO (AFM) projection.

[All assemblages contain quartz and muscovite]

| Metamorphic zone | Mineral assemblage | Metamorphic zone | Mineral assemblage |
|---|---|---|---|
| Biotite | Chlorite-biotite | Lower kyanite-biotite | Biotite-garnet |
| | | | Biotite-staurolite |
| Garnet | Chlorite-biotite | | Biotite-kyanite |
| | Biotite-garnet | | Biotite-garnet-staurolite |
| | Chlorite-biotite-garnet | | Biotite-staurolite-kyanite |
| | | | Biotite-garnet-staurolite-kyanite |
| Staurolite-biotite | Biotite | | |
| | Chlorite-biotite | | |
| | Biotite-garnet | Upper kyanite-biotite | Biotite-garnet |
| | Biotite-staurolite | | Biotite-kyanite |
| | Chlorite-biotite-garnet | | |
| | Biotite-garnet-staurolite | Sillimanite | Biotite-sillimanite |
| | Chlorite-biotite-garnet-staurolite | | Biotite-garnet-sillimanite |
| | | | Biotite-kyanite-sillimanite |

In the Juneau area, however, the absence of prograde chlorite in the staurolite-biotite zone, other than near the staurolite-biotite isograd, indicates that the first kyanite and the kyanite-biotite isograd did not form by reaction 4, an indication which is consistent with the recent observations elsewhere of Holdaway and others (1988). In the Juneau area the first appearance of kyanite occurs in garnet-bearing rocks, and the kyanite-biotite isograd can be attributed to the model discontinuous reaction

$$St+Ms+Qtz=Ky+Bt+Grt+H_2O \quad (5)$$

which is divariant in nature because the "four phase" assemblage staurolite-kyanite-biotite-garnet persists over a significant field interval. Kyanite+biotite can also be formed by the continuous reaction

$$St+Ms+Qtz=Ky+Bt+H_2O, \quad (6)$$

which yields rare biotite-staurolite-kyanite assemblages. Reaction 3 may also maintain equilibrium in the kyanite-biotite zone. The divariant reaction

$$St+Qtz=Ky+Grt+H_2O \quad (7)$$

is also possible, although the absence of kyanite-garnet assemblages without biotite suggests that bulk compositions were not appropriate for reaction 7.

The staurolite-out isograd can be modeled by either reaction 5 or 6 going to completion. The limiting assemblage kyanite-biotite-garnet has not been observed in muscovite-bearing rocks in the Juneau area, but it is common in muscovite-absent rocks, some with a trace of staurolite, which might represent reaction 5 going to completion in K-deficient rocks.

The absence of staurolite in sillimanite-bearing samples indicates that reactions 5 and 6 were completed before the reaction

$$Ky=Sil, \quad (8)$$

which defines the sillimanite isograd. With further increase in grade, garnet and muscovite react continuously to form sillimanite and biotite.

Changes in the Mg/(Mg+Fe) ratios of biotite and staurolite with increasing metamorphic grade in three- and four-phase assemblages appropriate to the above reactions are generally consistent with the changes predicted by Thompson (1976), although exceptions do exist. Changes in garnet composition in the same assemblages are further complicated owing to complex zoning patterns and retrograde equilibration of some rim compositions.

Himmelberg and others (1991) showed that the above sequence of reactions and the calculated pressure and temperature for the individual metamorphic zones are consistent with the petrogenetic grid of Spear and Cheney (1989) (fig. 4).

## MINERAL CHEMISTRY

Mineral analyses were obtained for 30 samples of quartz-muscovite-bearing pelitic schists and for 10 samples of muscovite-absent pelitic schists. Analyses of samples used for thermobarometry were previously reported by Himmelberg and others (1991). Additional analyses for low variance assemblages are given in tables 4 through 9; however, the mineral chemistry summary given below is based on all analyses. Analyses of garnet zonation and plagioclase were obtained using the JEOL model 733 superprobe at Washington University, St. Louis, Mo.; all other analyses were obtained using the ARL EMX-SM microprobe at the University of Missouri-Columbia. Matrix corrections were made by the method of Bence and Albee (1968) using the correction factors of Albee and Ray (1970). Owing to the presence of graphite and ilmenite in most samples, iron was assumed to be $Fe^{2+}$. Tabulated chlorite, muscovite, biotite, and staurolite analyses are averages of several grains per sample; plagioclase analyses are grain averages for unzoned samples and rim averages for zoned samples. Garnet core and rim or near-rim analyses were grouped and averaged

**Table 3.** Mineral associations and localities of samples of pelitic and semipelitic rocks obtained near Juneau, Alaska.

[In addition to the minerals listed, most assemblages contain graphite, tourmaline, and ilmenite. Beryl, allanite, zircon, sphene, and calcite may also be present. Chl, chlorite; Bt, biotite; Grt, garnet; St, staurolite; Ky, kyanite; Sil, sillimanite; Qtz, quartz; Ms, muscovite; Pl, plagioclase; X, mineral present; query (?), identification uncertain; space, mineral not detected. Where a mineral's presence is enclosed in brackets, it is interpreted to be a lower grade relict]

| Zone | Chl | Bt | Grt | St | Ky | Sil | Qtz | Ms | Pl | Quadrangle | Area | Latitude | Longitude | Sample No. |
|---|---|---|---|---|---|---|---|---|---|---|---|---|---|---|
| Bt | | X | | | | | X | X | | Juneau B2 | Heintzleman Ridge | 58° 22' 55" | 134° 30' 55" | 79GH1A |
| Bt | | X | | | | | X | X | X | Juneau B2 | Heintzleman Ridge | 58° 22' 53" | 134° 31' 10" | 79GH2A |
| Bt | | | | | | | X | X | | Juneau B2 | Heintzleman Ridge | 58° 22' 50" | 134° 31' 40" | 79GH4A |
| Bt | X | ? | | | | | X | X | X | Juneau B2 | Heintzleman Ridge | 58° 22" 34" | 134° 33' 05" | 79GH5A |
| Bt | X | X | | | | | X | X | | Juneau B2 | Heintzleman Ridge | 58° 23' 04" | 134° 30' 03" | 79GH11B |
| Bt | | X | | | | | X | X | | Juneau B2 | Blackerby Rridge | 58° 20' 40" | 134° 27' 37" | 79GH63A |
| Bt | X | X | | | | | X | | | Juneau B2 | Blackerby Ridge | 58° 21' 03" | 134° 27' 15" | 81GH19A |
| Bt | X | X | | | | | X | X | | Juneau B2 | Blackerby Ridge | 58° 21' 02" | 134° 27' 06" | 81GH20A |
| Bt | X | X | | | | | | | X | Juneau B1 | Sheep Mt. | 58° 17' 14" | 134° 19' 22" | 83DB93B |
| Bt | X | X | | | | | X | X | | Juneau B1 | Sheep Mt. | 58° 17' 20" | 134° 18' 50" | 83GH8A |
| Bt | | X | | | | | X | X | | Juneau B1 | Sheep Mt. | 58° 17' 23" | 134° 18' 34" | 83GH9A |
| Bt | X | X | | | | | X | X | X | Juneau B1 | Sheep Mt. | 58° 17' 23" | 134° 18' 34" | 83GH9B |
| Bt | | X | | | | | X | X | | Juneau B1 | Powerline Ridge | 58° 16' 46" | 134° 16' 39" | 83GH5A |
| Bt | | X | | | | | X | X | ? | Juneau B1 | Powerline Ridge | 58° 16' 41" | 134° 16' 42" | 83GH6A |
| Bt | | X | | | | | X | X | | Juneau B1 | Powerline Ridge | 58° 16' 38" | 134° 16' 22" | 83SK93A |
| Bt | X | X | | | | | X | | ? | Juneau B1 | Powerline Ridge | 58° 16' 45" | 134° 16' 20" | 83SK94A |
| Bt | | X | | | | | X | X | | Juneau B1 | Hawthorne Peak | 58° 16' 09" | 134° 15' 35" | 83GH19A |
| Bt | | X | | | | | X | | | Juneau A1 | Taku Inlet | 58° 11' 24" | 134° 05' 05" | 84SK262D |
| Bt | | X | | | | | | | | Juneau A1 | Taku Inlet | 58° 11' 20" | 134° 05' 11" | 84SK263A |
| Bt | | X | | | | | X | X | X | Juneau A1 | Taku Inlet | 58° 11' 10" | 134° 05' 17" | 84SK265A |
| Bt | X | X | | | | | X | X | X | Juneau A1 | Taku Inlet | 58° 10' 47" | 134° 05' 15" | 84SK267A |
| Bt | X | X | | | | | X | X | X | Juneau A1 | Taku Inlet | 58° 10' 33" | 134° 05' 09" | 84SK268A |
| Grt | | X | X | | | | X | X | | Juneau B2 | Heintzleman Ridge | 58° 23' 37" | 134° 30' 00" | 79GH15A |
| Grt | X | X | | | | | X | X | | Juneau B2 | Heintzleman Ridge | 58° 23' 52" | 134° 29' 57" | 79GH17A |
| Grt | | X | | | | | X | X | | Juneau B2 | Heintzleman Ridge | 58° 23' 26" | 134° 29' 14" | 79GH19A |
| Grt | | X | X | | | | X | X | ? | Juneau B2 | Heintzleman Ridge | 58° 23' 27" | 134° 29' 05" | 79GH20A |
| Grt | | X | X | | | | X | X | X | Juneau B2 | Heintzleman Ridge | 58° 23' 27" | 134° 29' 05" | 79GH20B |
| Grt | | X | X | | | | X | X | X | Juneau B2 | Heintzleman Ridge | 58° 23' 17" | 134° 29' 40" | 81DB15A |
| Grt | X | X | X | | | | X | X | | Juneau B2 | Heintzleman Ridge | 58° 23' 19" | 134° 29' 48" | 81DB16A |
| Grt | | X | X | | | | X | X | X | Juneau B2 | Heintzleman Ridge | 58° 23' 19" | 134° 29' 48" | 81DB16B |
| Grt | X | X | | | | | X | X | X | Juneau B2 | Heintzleman Ridge | 58° 23' 30" | 134° 29' 56" | 81DB19A |
| Grt | | X | | | | | X | X | | Juneau B2 | Heintzleman Ridge | 58° 23' 30" | 134° 29' 56" | 81DB19B |
| Grt | X | X | | | | | X | X | | Juneau B2 | Heintzleman Ridge | 58° 23' 45" | 134° 29' 59" | 81DB20A |
| Grt | X | X | | | | | X | X | | Juneau B2 | Blackerby Ridge | 58° 21' 05" | 134° 26' 59" | 81GH18A |
| Grt | | X | X | | | | X | X | | Juneau B2 | Blackerby Ridge | 58° 21' 10" | 134° 26' 28 " | 81GH21A |
| Grt | X | X | X | | | | X | X | | Juneau B2 | Blackerby Ridge | 58° 21' 10" | 134° 26' 28" | 81GH21B |
| Grt | X | X | X | | | | X | X | | Juneau B1 | Sheep Mt. | 58° 17' 34" | 134° 17' 56" | 83DB89B |
| Grt | | X | X | | | | X | X | | Juneau B1 | Sheep Mt. | 58° 17' 25" | 134° 18' 20" | 83GH10A |
| Grt | X | X | | | | | X | X | X | Juneau B1 | Sheep Mt. | 58°17' 32" | 134° 18' 10" | 83GH11A |
| Grt | | X | | | | | X | X | X | Juneau B1 | Sheep Mt. | 58° 17' 30" | 134° 17' 17" | 83GH12A |
| Grt | | X | | | | | X | X | X | Juneau B1 | Sheep Mt. | 58°1 7' 27" | 134° 17' 05" | 83GH13B |
| Grt | X | X | | | | | X | X | | Juneau B1 | Powerline Ridge | 58° 16' 55" | 134° 16' 35" | 83GH2A |
| Grt | | X | X | | | | X | X | | Juneau B1 | Powerline Ridge | 58° 16' 56" | 134° 16' 40" | 83GH3A |
| Grt | | X | X | | | | X | X | | Juneau B1 | Powerline Ridge | 58° 16' 53" | 134° 16' 43" | 83GH4A |
| Grt | X | X | | | | | X | X | | Juneau B1 | Powerline Ridge | 58° 16' 49" | 134° 16' 14" | 83SK95A |
| Grt | | X | X | | | | X | X | | Juneau B1 | Hawthorne Peak | 58° 16' 14" | 134° 15' 22" | 83GH20A |
| Grt | | X | | | | | X | X | | Juneau B1 | Hawthorne Peak | 58° 16' 23" | 134° 14' 56" | 83GH21A |
| Grt | | X | X | | | | X | X | X | Juneau A1 | Taku Inlet | 58° 11' 39" | 134° 04' 52" | 84SK270A |
| Grt | | X | | | | | X | | X | Juneau A1 | Taku Inlet | 58° 11' 39" | 134° 04' 52" | 84SK270C |
| Grt | | X | | | | | X | X | X | Juneau A1 | Taku Inlet | 58° 11' 55" | 134° 04' 49" | 84SK272A |
| Grt | | X | | | | | X | X | X | Juneau A1 | Taku Inlet | 58° 12' 38" | 134° 07' 52" | 85GH66A |
| St-Bt | | X | X | X | | | X | X | | Juneau B2 | Heintzleman Ridge | 58° 23' 29" | 134° 29' 00" | 79GH21A |
| St-Bt | | X | X | | | | X | X | | Juneau B2 | Heintzleman Ridge | 58° 23' 29" | 134° 29' 00" | 79GH21B |
| St-Bt | | X | X | X | | | X | X | | Juneau B2 | Heintzleman Ridge | 58° 23' 31" | 134° 28' 57" | 79GH22A |
| St-Bt | X | X | X | X | | | X | X | X | Juneau B2 | Heintzleman Ridge | 58° 23' 30" | 134° 29' 00" | 81SK11A |
| St-Bt | X | X | | | | | X | X | | Juneau B2 | Heintzleman Ridge | 58° 23' 30" | 134° 29' 00" | 81SK11B |
| St-Bt | X | X | X | | | | X | X | | Juneau B2 | Heintzleman Ridge | 58° 23' 40" | 134° 29' 00" | 81SK12A |
| St-Bt | | X | X | | | | X | X | X | Juneau B2 | Heintzleman Ridge | 58° 23' 35" | 134° 28' 50" | 81SK13A |
| St-Bt | | X | X | | | | X | X | | Juneau B2 | Heintzleman Ridge | 58° 23' 28" | 134° 28' 50" | 81GH5A |
| St-Bt | | X | X | X | | | X | X | | Juneau B2 | Heintzleman Ridge | 58° 23' 28" | 134° 28' 50" | 81GH5B |
| St-Bt | | X | X | X | | | X | X | | Juneau B2 | Heintzleman Ridge | 58° 23' 28" | 134° 28' 50" | 81GH5C |
| St-Bt | X | X | X | X | | | X | X | | Juneau B2 | Blackerby Ridge | 58° 21' 10" | 134° 26' 25" | 79GH57A |
| St-Bt | X | X | | | | X | X | | | Juneau B2 | Blackerby Ridge | 58° 21' 09" | 134° 26' 30" | 79GH58A |
| St-Bt | | X | X | | | | X | X | | Juneau B2 | Blackerby Ridge | 58° 21' 09" | 134° 26' 30" | 79GH58B |
| St-Bt | | X | X | | | | X | X | X | Juneau B2 | Blackerby Ridge | 58° 21' 17" | 134° 26' 04" | 79GH84B |
| St-Bt | | X | X | | | | X | | X | Juneau B2 | Blackerby Ridge | 58° 21' 17" | 134° 26' 04" | 79GH84C |
| St-Bt | | X | | | | | X | X | X | Juneau B2 | Blackerby Ridge | 58° 21' 20" | 134° 25' 55" | 79GH85A |
| St-Bt | | X | X | X | X | | X | X | X | Juneau B2 | Blackerby Ridge | 58° 21' 30" | 134° 24' 49" | 81DB21A |
| St-Bt | | X | | | | | X | X | X | Juneau B2 | Blackerby Ridge | 58° 21' 21" | 134° 25' 45" | 81GH23A |
| St-Bt | X | X | X | | | | X | X | X | Juneau B2 | Blackerby Ridge | 58° 21' 22" | 134° 25' 38" | 81GH24A |
| St-Bt | | X | | X | | | X | X | ? | Juneau B1 | Powerline Ridge | 58° 16' 49" | 134° 16' 14" | 83GH7A |
| St-Bt | | X | | | | | X | X | | Juneau B1 | Powerline Ridge | 58° 17' 07" | 134° 16' 35" | 83GH14A |
| St-Bt | | X | X | | | | X | | X | Juneau B1 | Powerline Ridge | 58° 17' 08" | 134° 15' 53" | 83GH15B |
| St-Bt | | X | X | | | | | X | | Juneau B1 | Powerline Ridge | 58° 17' 08" | 134° 15' 53 " | 83GH15C |

**Table 3.** Mineral associations and localities of samples of pelitic and semipelitic rocks obtained near Juneau, Alaska—Continued.

| Zone | Chl | Bt | Grt | St | Ky | Sil | Qtz | Ms | Pl | Quadrangle | Area | Latitude | Longitude | Sample No. |
|---|---|---|---|---|---|---|---|---|---|---|---|---|---|---|
| St-Bt | | X | | | | | X | X | X | Juneau B1 | Powerline Ridge | 58° 17' 12" | 134° 15' 43" | 83GH16A |
| St-Bt | | X | | | | | X | X | X | Juneau B1 | Powerline Ridge | 58° 17' 12" | 134° 15' 43" | 83GH16B |
| St-Bt | | X | X | | | | X | X | X | Juneau B1 | Powerline Ridge | 58° 17' 39" | 134° 15' 21" | 84GH18A |
| St-Bt | | X | X | | | | X | X | X | Juneau B1 | Powerline Ridge | 58° 17' 39" | 134° 15' 21" | 83GH18B |
| St-Bt | ? | X | X | X | | | X | X | | Juneau B1 | Powerline Ridge | 58° 16' 46" | 134° 15' 40" | 83GH22A |
| St-Bt | | X | X | | | | X | X | X | Juneau B1 | Powerline Ridge | 58° 17' 28" | 134° 14' 55" | 83GH28A |
| St-Bt | | X | | X | | | X | X | | Juneau B1 | Hawthorne Peak | 58° 16' 22" | 134° 14' 37" | 83GH24B |
| St-Bt | | X | | | | | X | X | | Juneau B1 | Hawthorne Peak | 58° 16' 00" | 134° 13' 00" | 84SK254A |
| St-Bt | | X | X | | | | X | X | X | Juneau B1 | Hawthorne Peak | 58° 16' 00" | 134° 12' 58" | 84SK254C |
| St-Bt | X | X | X | X | | | X | | X | Juneau B1 | Hawthorne Peak | 58° 15' 55" | 134° 12' 01" | 84SK256A |
| St-Bt | | X | | | | | X | X | X | Juneau B1 | Hawthorne Peak | 58° 15' 55" | 134° 12' 01" | 84SK256B |
| St-Bt | | X | | | | | X | X | X | Juneau B1 | Hawthorne Peak | 58° 15' 55" | 134° 12' 01" | 84SK256C |
| St-Bt | | X | | | | | X | X | X | Juneau B1 | Hawthorne Peak | 58° 15' 54" | 134° 11' 42" | 84SK257A |
| St-Bt | | X | | | | | X | X | X | Juneau B1 | Hawthorne Peak | 58° 15' 54" | 134° 11' 42" | 84SK257B |
| St-Bt | | X | X | | | | X | X | X | Juneau B1 | Hawthorne Peak | 58° 15' 58" | 134° 11' 28" | 84SK258A |
| St-Bt | | X | | | | | X | X | X | Juneau B1 | Hawthorne Peak | 58° 16' 22" | 134° 10' 16" | 84SK261B |
| St-Bt | X | X | | X | | | X | X | | Juneau A1 | Taku Inlet | 58° 14' 40" | 134° 10' 07" | 84GH25A |
| St-Bt | ? | X | X | X | | | X | X | | Juneau A1 | Taku Inlet | 58° 14' 40" | 134° 10' 07" | 84GH25B |
| St-Bt | | X | | X | | | X | X | X | Juneau A1 | Taku Inlet | 58° 14' 40" | 134° 10' 07" | 84GH25C |
| St-Bt | X | X | | | | | X | X | | Juneau A1 | Taku Inlet | 58° 14' 17" | 134° 10' 08" | 84SK253A |
| St-Bt | X | X | | X | | | X | X | X | Juneau A1 | Taku Inlet | 58°13' 20" | 134 ° 08' 26" | 85GH67A |
| St-Bt | X | X | | X | | | X | X | X | Juneau A1 | Taku Inlet | 58° 13' 20" | 134° 08' 26" | 85GH67B |
| St-Bt | | X | | X | | | X | X | X | Juneau A1 | Taku Inlet | 58° 13' 20" | 134° 08' 26" | 85GH67C |
| St-Bt | X | X | | | | | X | X | X | Juneau A1 | Taku Inlet | 58° 13' 35" | 134° 08' 15" | 85GH68A |
| St-Bt | | X | | | | | X | X | X | Juneau A1 | Taku Inlet | 58° 13' 57" | 134° 07' 15" | 85GH69A |
| St-Bt | | X | | | | | X | X | | Juneau A1 | Taku Inlet | 58° 13' 57" | 134° 07' 15" | 85GH69B |
| Ky-Bt | | X | | | | | X | X | X | Juneau B2 | Heintzleman Ridge | 58° 23' 34" | 134° 28' 50" | 79GH23A |
| Ky-Bt | | X | X | X | X | | X | X | X | Juneau B2 | Heintzleman Ridge | 58° 23' 34" | 134° 28' 50" | 79GH23B |
| Ky-Bt | | X | | X | | | X | X | X | Juneau B2 | Heintzleman Ridge | 58° 23' 39" | 134° 28' 43" | 79GH24A |
| Ky-Bt | | X | X | X | | | X | X | | Juneau B2 | Heintzleman Ridge | 58° 23' 42" | 134° 28' 41" | 79GH25A |
| Ky-Bt | | X | X | X | | | X | X | | Juneau B2 | Heintzleman Ridge | 58° 23' 42" | 134° 28' 41" | 79GH25B |
| Ky-Bt | | X | X | X | | | X | X | | Juneau B2 | Heintzleman Ridge | 58° 23' 42" | 134° 28' 41" | 79GH25C |
| Ky-Bt | | X | | | | | X | X | | Juneau B2 | Heintzleman Ridge | 58° 23' 47" | 134° 28' 34 " | 79GH27A |
| Ky-Bt | | X | X | | | | X | X | X | Juneau B2 | Heintzleman Ridge | 58° 23' 48" | 134° 28' 25" | 79GH28A |
| Ky-Bt | | X | X | | | | X | | X | Juneau B2 | Heintzleman Ridge | 58° 23' 55" | 134° 28' 12" | 79GH30A |
| Ky-Bt | | X | | | | | X | | X | Juneau B2 | Heintzleman Ridge | 58° 23' 55" | 134° 28' 12" | 79GH30B |
| Ky-Bt | | X | X | | | | X | X | X | Juneau B2 | Heintzleman Ridge | 58° 23' 54" | 134° 28' 07" | 79GH31A |
| Ky-Bt | | X | X | | | | X | X | X | Juneau B2 | Heintzleman Ridge | 58° 23' 53" | 134° 28' 03" | 79GH32A |
| Ky-Bt | | X | X | | | | X | X | X | Juneau B2 | Heintzleman Ridge | 58° 23' 54" | 134° 28' 00" | 79GH33A |
| Ky-Bt | | X | X | | | | X | X | X | Juneau B2 | Heintzleman Ridge | 58° 23' 56" | 134° 27' 57" | 79GH34A |
| Ky-Bt | | X | X | X | X | | X | X | X | Juneau B2 | Heintzleman Ridge | 58° 23' 58" | 134° 27' 44" | 79GH35A |
| Ky-Bt | | X | X | | | | X | | X | Juneau B2 | Heintzleman Ridge | 58° 24' 01" | 134° 27' 35" | 79GH36A |
| Ky-Bt | | X | X | | | | X | | X | Juneau B2 | Heintzleman Ridge | 58° 24' 02" | 134° 27' 23" | 79GH38A |
| Ky-Bt | | X | | | | | X | X | X | Juneau B2 | Heintzleman Ridge | 58° 24' 02" | 134° 27' 23" | 79GH38B |
| Ky-Bt | | X | X | | | | X | | X | Juneau B2 | Heintzleman Ridge | 58° 24' 08" | 134° 26' 55" | 79GH41A |
| Ky-Bt | | X | X | | | | X | | X | Juneau B2 | Heintzleman Ridge | 58° 24' 09" | 134° 26' 42" | 79GH42A |
| Ky-Bt | | X | X | | | | X | | X | Juneau B2 | Heintzleman Ridge | 58° 24' 13" | 134° 26' 29" | 79GH43B |
| Ky-Bt | | X | X | | | | X | | X | Juneau B2 | Heintzleman Ridge | 58° 24' 15" | 134° 26' 25" | 79GH44A |
| Ky-Bt | | X | X | | | | X | X | X | Juneau B2 | Heintzleman Ridge | 58° 24' 16" | 134° 26' 20" | 79GH45A |
| Ky-Bt | | X | X | X | | | X | X | | Juneau B2 | Heintzleman Ridge | 58° 23'33" | 134° 28' 35" | 81GH6A |
| Ky-Bt | | X | X | X | | | X | X | | Juneau B2 | Heintzleman Ridge | 58° 23' 33" | 134° 28' 35" | 81GH6B |
| Ky-Bt | | X | X | X | X | | X | | | Juneau B2 | Heintzleman Ridge | 58° 23' 33" | 134° 28' 35" | 81GH6C |
| Ky-Bt | | X | X | X | X | | X | X | | Juneau B2 | Heintzleman Ridge | 58° 23' 43" | 134° 28' 06" | 81GH7A |
| Ky-Bt | | X | X | X | X | | X | X | | Juneau B2 | Heintzleman Ridge | 58° 23' 43" | 134° 28' 06" | 81GH7B |
| Ky-Bt | | X | X | | | | X | X | X | Juneau B2 | Heintzleman Ridge | 58° 23' 42" | 134° 28' 22" | 81GH8A |
| Ky-Bt | | X | | | | | X | X | X | Juneau B2 | Heintzleman Ridge | 58° 23' 51" | 134° 28' 00" | 81GH10A |
| Ky-Bt | | X | X | | | | X | X | X | Juneau B2 | Heintzleman Ridge | 58° 23' 55" | 134° 27' 59" | 81GH11A |
| Ky-Bt | | X | X | | | | X | X | X | Juneau B2 | Heintzleman Ridge | 58° 24' 00" | 134° 27' 41" | 81GH13A |
| Ky-Bt | | X | X | X | X | | X | X | | Juneau B2 | Heintzleman Ridge | 58° 23' 59" | 134° 27' 39" | 81GH14A |
| Ky-Bt | | X | X | X | X | | X | X | X | Juneau B2 | Heintzleman Ridge | 58° 23' 59" | 134° 27' 39" | 81GH14B |
| Ky-Bt | | X | X | | X | | X | | X | Juneau B2 | Heintzleman Ridge | 58° 24' 07" | 134° 27' 07" | 81GH15A |
| Ky-Bt | | X | X | | | | X | | X | Juneau B2 | Heintzleman Ridge | 58° 24' 07" | 134° 27' 07" | 81GH15B |
| Ky-Bt | | X | X | | X | | X | | X | Juneau B2 | Heintzleman Ridge | 58° 24' 08" | 134° 27' 03" | 81GH16A |
| Ky-Bt | | X | X | | X | | X | | X | Juneau B2 | Heintzleman Ridge | 58° 24' 08" | 134° 27' 03" | 81GH16B |
| Ky-Bt | | X | | | | | | X | X | Juneau B2 | Heintzleman Ridge | 58° 24' 10" | 134° 26' 51" | 81GH17A |
| Ky-Bt | | X | X | | | | X | | X | Juneau B2 | Heintzleman Ridge | 58° 24' 10" | 134° 26' 51" | 81GH17B |
| Ky-Bt | | X | X | | | | X | X | | Juneau B2 | Heintzleman Ridge | 58° 23' 45" | 134° 28' 45" | 81SK14A |
| Ky-Bt | | X | | | | | X | X | | Juneau B2 | Heintzleman Ridge | 58° 23' 45" | 134° 28' 45" | 81SK14B |
| Ky-Bt | | X | X | X | ? | | X | X | | Juneau B2 | Heintzleman Ridge | 58° 23' 45" | 134° 28' 45" | 81SK14C |
| Ky-Bt | | X | X | X | | | X | X | | Juneau B2 | Heintzleman Ridge | 58° 23' 55" | 134° 29' 50" | 81SK15A |
| Ky-Bt | | X | X | | | | X | X | | Juneau B2 | Heintzleman Ridge | 58° 24' 00" | 134° 29' 50" | 81SK16A |
| Ky-Bt | | X | X | | | | X | X | | Juneau B2 | Heintzleman Ridge | 58° 24' 00" | 134° 29' 50" | 81SK16B |
| Ky-Bt | | X | X | X | X | | X | X | | Juneau B2 | Heintzleman Ridge | 58° 24' 05" | 134° 29' 40" | 81SK17A |
| Ky-Bt | | X | X | X | X | | X | X | | Juneau B2 | Heintzleman Ridge | 58° 24' 05" | 134° 29' 40" | 81SK17B |

**Table 3.** Mineral associations and localities of samples of pelitic and semipelitic rocks obtained near Juneau, Alaska—Continued.

| Zone | Chl | Bt | Grt | St | Ky | Sil | Qtz | Ms | Pl | Quadrangle | Area | Latitude | Longitude | Sample No. |
|---|---|---|---|---|---|---|---|---|---|---|---|---|---|---|
| Ky-Bt--- | | X | | | | | X | X | X | Juneau B2 | Heintzleman Ridge | 58° 24' 15" | 134° 29' 20" | 81SK19A |
| Ky-Bt--- | | X | X | | | | X | X | X | Juneau B2 | Heintzleman Ridge | 58° 24' 00" | 134° 29' 10" | 81SK20A |
| Ky-Bt--- | | X | | X | X | | X | X | X | Juneau B2 | Heintzleman Ridge | 58° 23' 50" | 134° 28' 50" | 81SK22A |
| Ky-Bt--- | | X | X | | | | X | | X | Juneau B2 | Blackerby Ridge | 58° 21' 23" | 134° 23' 18" | 79GH78A |
| Ky-Bt--- | | X | | | | | X | | X | Juneau B2 | Blackerby Ridge | 58° 21' 23" | 134° 23' 18" | 79GH78B |
| Ky-Bt--- | | X | X | | | | X | | X | Juneau B2 | Blackerby Ridge | 58° 21' 18" | 134° 23' 55" | 79GH80A |
| Ky-Bt--- | | X | X | | | | X | X | X | Juneau B2 | Blackerby Ridge | 58° 21' 16" | 134° 24' 03" | 79GH81C |
| Ky-Bt--- | | X | X | | | | | X | X | Juneau B2 | Blackerby Ridge | 58° 21' 15" | 134° 24' 25" | 79GH82A |
| Ky-Bt--- | | X | X | | | | X | X | X | Juneau B2 | Blackerby Ridge | 58° 21' 17" | 134° 24' 29" | 79GH83A |
| Ky-Bt--- | | X | X | | | | X | | X | Juneau B2 | Blackerby Ridge | 58° 21' 23" | 134° 25' 35" | 79GH88A |
| Ky-Bt--- | | X | X | | | | X | | X | Juneau B2 | Blackerby Ridge | 58° 21' 23" | 134° 25' 35" | 79GH88B |
| Ky-Bt--- | | X | X | | | | X | X | X | Juneau B2 | Blackerby Ridge | 58° 21' 23" | 134° 25' 35" | 79GH88C |
| Ky-Bt--- | | X | X | X | X | | X | X | X | Juneau B2 | Blackerby Ridge | 58° 21' 23" | 134° 25' 35" | 79GH88D |
| Ky-Bt--- | | X | X | X | X | | X | X | X | Juneau B2 | Blackerby Ridge | 58° 21' 24" | 134° 25' 30" | 79GH89A |
| Ky-Bt--- | | X | X | X | X | | X | X | X | Juneau B2 | Blackerby Ridge | 58° 21' 24" | 134° 25' 30" | 79GH89B |
| Ky-Bt--- | | X | X | | | | X | X | X | Juneau B2 | Blackerby Ridge | 58° 21' 21" | 134° 24' 58" | 79GH91A |
| Ky-Bt--- | | X | X | X | X | | X | | X | Juneau B2 | Blackerby Ridge | 58° 21' 17" | 134° 24' 30" | 79GH92A |
| Ky-Bt--- | | X | | X | X | | | | X | Juneau B2 | Blackerby Ridge | 58° 21' 18" | 134° 24' 36" | 79GH93A |
| Ky-Bt--- | | X | X | X | X | | X | X | X | Juneau B2 | Blackerby Ridge | 58° 21' 38" | 134° 24' 45" | 81DB22A |
| Ky-Bt--- | | X | X | | X | X | X | X | X | Juneau B2 | Blackerby Ridge | 58° 21' 38" | 134° 24' 45" | 81DB22C |
| Ky-Bt--- | | X | X | | X | X | X | | X | Juneau B2 | Blackerby Ridge | 58° 21' 45" | 134° 24' 41" | 81DB23A |
| Ky-Bt--- | | X | X | | | | X | | X | Juneau B2 | Blackerby Ridge | 58° 21' 47" | 134° 24' 33" | 81DB24A |
| Ky-Bt--- | | X | X | | | | | X | X | Juneau B2 | Blackerby Ridge | 58° 21' 48" | 134° 24' 26" | 81DB25A |
| Ky-Bt--- | | X | X | | | | X | | X | Juneau B2 | Blackerby Ridge | 58° 22' 05" | 134° 24' 07" | 81DB27A |
| Ky-Bt--- | | X | X | | | | X | | X | Juneau B2 | Blackerby Ridge | 58° 21' 46" | 134° 23' 19" | 81DB32A |
| Ky-Bt--- | | X | X | | | | X | | X | Juneau B2 | Blackerby Ridge | 58° 21' 38" | 134° 23' 04" | 81DB33A |
| Ky-Bt--- | | X | X | X | X | | X | X | X | Juneau B2 | Blackerby Ridge | 58° 21' 24" | 134° 25' 30" | 81GH25A |
| Ky-Bt--- | | X | X | | | | X | | X | Juneau B2 | Blackerby Ridge | 58° 21' 20" | 134° 23' 20" | 81SK29A |
| Ky-Bt--- | | X | X | | | | X | | X | Juneau B2 | Blackerby Ridge | 58° 21' 20" | 134° 23' 20" | 81SL29B |
| Ky-Bt--- | | X | X | | | | X | | X | Juneau B2 | Blackerby Ridge | 58° 21' 20" | 134° 23' 50" | 81SK31A |
| Ky-Bt--- | | X | | | | | X | | X | Juneau B2 | Blackerby Ridge | 58° 21' 15" | 134° 24' 20" | 81SK32A |
| Ky-Bt--- | | X | | | X | | X | X | X | Juneau B2 | Blackerby Ridge | 58° 21' 17" | 134° 24' 35" | 81SK33A |
| Sil------- | | X | X | | [X] | X | X | | X | Juneau B2 | Heintzleman Ridge | 58° 24' 18" | 134° 26' 19" | 79GH46A |
| Sil------- | | X | X | | [X] | X | X | | X | Juneau B2 | Heintzleman Ridge | 58° 24' 18" | 134° 26' 19" | 79GH46B |
| Sil------- | | X | X | | [X] | X | X | | X | Juneau B2 | Heintzleman Ridge | 58° 24' 20" | 134° 26' 11" | 79GH47A |
| Sil------- | | X | X | | | X | X | | X | Juneau B2 | Heintzleman Ridge | 58° 24' 20" | 134° 26' 11" | 79GH47B |
| Sil------- | | X | X | | [X] | X | X | | X | Juneau B2 | Heintzleman Ridge | 58° 24' 28" | 134° 26' 02" | 79GH49B |
| Sil------- | | X | X | | | | X | | X | Juneau B2 | Heintzleman Ridge | 58° 24' 33" | 134° 25' 58" | 79GH50A |
| Sil------- | | X | X | | [X] | X | X | X | X | Juneau B2 | Heintzleman Ridge | 58° 24' 40" | 134° 25' 57" | 79GH51A |
| Sil------- | | X | X | | | X | X | X | X | Juneau B2 | Heintzleman Ridge | 58° 24' 40" | 134° 25' 57" | 79GH51B |
| Sil------- | | X | X | | | X | X | X | X | Juneau B2 | Heintzleman Ridge | 58° 24' 47" | 134° 25' 55" | 79GH52A |
| Sil------- | | X | | | | X | X | X | X | Juneau B2 | Heintzleman Ridge | 58° 24' 47" | 134° 25' 55" | 79GH52B |
| Sil------- | | X | | | | | | X | | Juneau B2 | Heintzleman Ridge | 58° 24' 57" | 134° 25' 27" | 79GH94A |
| Sil------- | | X | X | | | | X | | X | Juneau B2 | Heintzleman Ridge | 58° 24' 56" | 134° 24' 31" | 79GH99A |
| Sil------- | | X | X | | | X | X | | X | Juneau B2 | Heintzleman Ridge | 58° 24' 57" | 134 24 21 | 79GH100B |
| Sil------- | | X | X | | | | X | | X | Juneau B2 | Blackerby Ridge | 58° 21' 31" | 134 22 00 | 79GH67A |
| Sil------- | | X | X | | | | X | | X | Juneau B2 | Blackerby Ridge | 58° 21' 31" | 134° 22' 00" | 79GH67B |
| Sil------- | | X | X | | | | X | | X | Juneau B2 | Blackerby Ridge | 58° 21' 32" | 134° 22' 39" | 79GH71B |
| Sil------- | | X | | | | | X | | X | Juneau B2 | Blackerby Ridge | 58° 21' 28" | 134° 22' 47" | 79GH73A |
| Sil------- | | X | | | | X | X | | X | Juneau B2 | Blackerby Ridge | 58° 21' 27" | 134° 22' 50" | 79GH74A |
| Sil------- | | X | X | | | | X | X | X | Juneau B2 | Blackerby Ridge | 58° 21' 26" | 134° 22' 51" | 79GH75A |
| Sil------- | | X | | | X | | X | X | X | Juneau B2 | Blackerby Ridge | 58° 21' 25" | 134° 23' 00" | 79GH76A |
| Sil------- | | X | X | | X | | X | | X | Juneau B2 | Blackerby Ridge | 58° 21' 25" | 134° 23' 00" | 79GH76B |
| Sil------- | | X | | | | X | X | | X | Juneau B2 | Blackerby Ridge | 58° 21' 25" | 134° 23' 00" | 79GH76C |
| Sil------- | | X | | | X | | X | X | X | Juneau B2 | Blackerby Ridge | 58° 21' 24" | 134° 23' 04" | 79GH77A |
| Sil------- | | X | | | | X | X | | X | Juneau B2 | Blackerby Ridge | 58° 21' 24" | 134° 23' 04" | 79GH77B |
| Sil------- | | X | | | | X | X | X | X | Juneau B2 | Blackerby Ridge | 58° 21' 05" | 134° 22' 30" | 81SK23C |
| Sil------- | | X | | | | | X | | X | Juneau B2 | Blackerby Ridge | 58° 21' 55" | 134° 23' 05" | 81SK24A |
| Sil------- | | X | X | | | | X | | X | Juneau B2 | Blackerby Ridge | 58° 21' 25" | 134° 22' 55" | 81SK27A |
| Sil------- | | X | X | | [X] | X | X | X | X | Juneau B2 | Blackerby Ridge | 58° 21' 25" | 134° 23' 10" | 81SK28A |

on the basis of chemical similarity; obvious rim retrograde analyses were not included.

Prograde chlorite coexisting with quartz, white mica, biotite, and plagioclase was analyzed in two samples from the low-grade biotite zone (table 4). Mg/(Mg+Fe) ratios are 0.52 and 0.67, and (Fe, Mg)/Al ratios are 1.76 and 1.67. There are no significant differences in composition from grain to grain in the same sample. Late-generation chlorite in a sample from the staurolite-biotite zone has an Mg/(Mg+Fe) ratio of 0.55 and an (Fe, Mg)/Al ratio of 1.57.

Plagioclase is present in most of the pelitic schists, and plagioclase analyses are given in table 5. The composition ranges from about $An_{12}$ to $An_{40}$ and shows no relation to metamorphic grade. Compositionally zoned plagioclase grains are not common; where zoning is present the rims are enriched by 1 to 5 mole percent in the anorthite component. Orthoclase content does not exceed 2.5 mole percent and commonly is less than 1 mole percent.

Muscovite in a given sample is chemically homogeneous, but the fact that its composition shows considerable

variation between samples appears to reflect bulk rock composition rather than systematic changes with metamorphic grade (table 6). Phengite content, expressed by excess Si over the ideal trisilicic formula, ranges from Si=3.01 to Si=3.16 per 11 oxygens, and paragonite content (Na/(K+Na+Ba)) ranges from about 0.08 to 0.29. Many Juneau area muscovites have a high Ba content; Ba/(K+Na+Ba) ratio ranges from about 0.01 to about 0.16, which is considerably higher than reported in other common pelitic schists (Guidotti, 1984).

Staurolite was analyzed in nine samples, four of which are given in table 7. Problems of the staurolite formula were discussed by Zen (1981) and Holdaway and others (1988). We calculated cation proportions on the basis of 23 oxygens, assuming 1 mole $H_2O$ per formula. The addition of $H_2O$ would increase the analytical sums to close to 100 percent. The Mg/(Mg+Fe) ratio ranges only from 0.17 to 0.23 in eight of the analyzed samples; one sample has an Mg/(Mg+Fe) ratio of 0.28. ZnO content ranges from 0.17 to 3.85 weight percent. No optical zoning of staurolite was noted, and the microprobe analyses show no appreciable chemical variation within grains or between grains in the same sample.

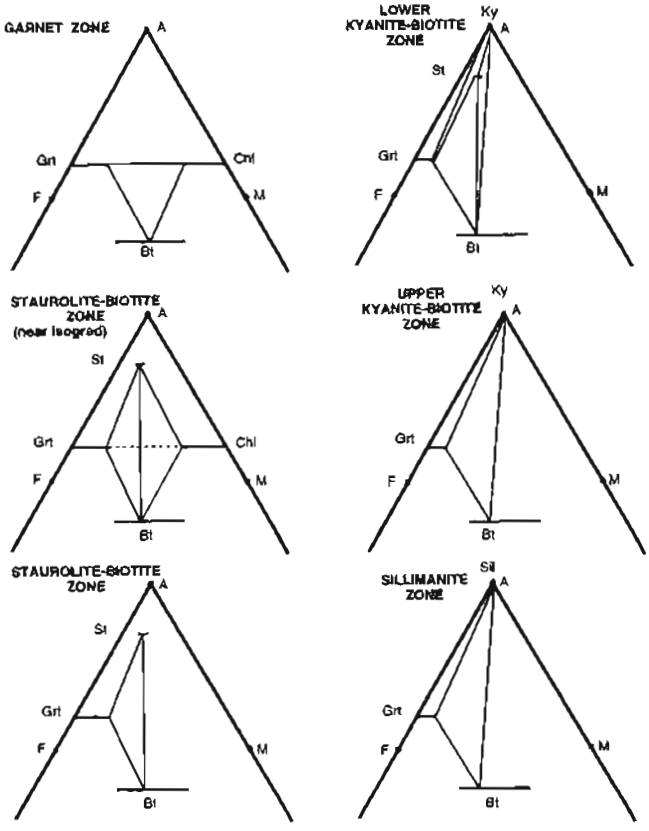


**Figure 3.** Schematic $Al_2O_3$-FeO-MgO (AFM) projections based on observed mineral assemblages in Juneau area. All assemblages include quartz and muscovite. A, $Al_2O_3$; F, FeO; M, MgO; Grt, garnet; Bt, biotite; Chl, chlorite; St, staurolite; Ky, kyanite; Sil, sillimanite (from Himmelberg and others, 1991).

Biotite analyses are given in table 8. Structural formulas of biotite calculated on the basis of 11 oxygens consistently yield an octahedral site occupancy of less than 3 and an A-site occupancy of less than 1. Dymek (1983) demonstrated that octahedral occupancy in biotite is generally less than 3 cations per formula as a result of Ti and $Al^{VI}$ octahedral substitution not balanced by tetrahedral Al. Biotite ranges in Mg/(Mg+Fe) ratio from 0.31 to 0.70. Many of the analyzed biotites occur in multivariant assemblages and the compositional variations clearly reflect bulk composition. In assemblages that are divariant relative to the ideal AFM projection, the biotite commonly changes in Mg/(Mg+Fe) ratio with metamorphic grade, consistent with the change predicted by Thompson (1976). In some instances, however, the variation between

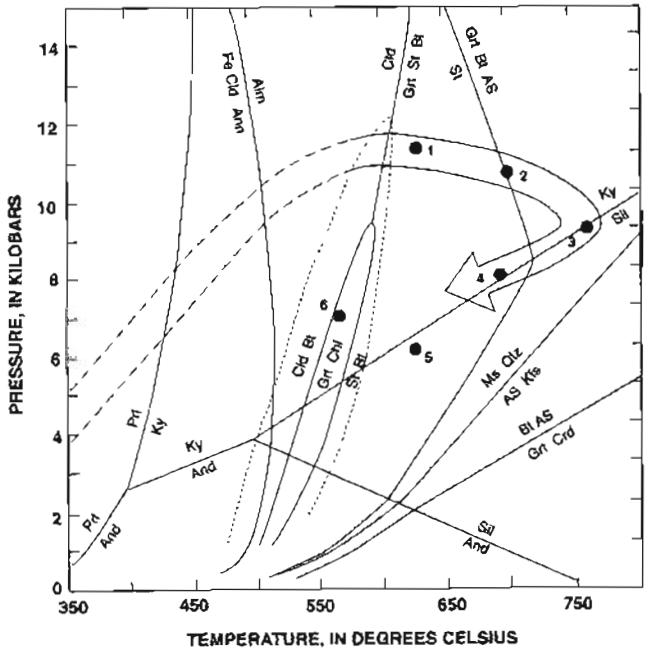


**Figure 4.** Petrogenetic grid for the $SiO_2$-$Al_2O_3$-FeO-MgO-$K_2O$-$H_2O$ system from Spear and Cheney (1989) showing reaction curves appropriate for assemblages in Juneau pelitic schists. Short-dashed boundaries are for garnet+chlorite+biotite assemblages where Mn/(Mn+Fe+Mg) is 0.1. Plotted points are preferred temperatures and pressures calculated from mineral equilibria for: lower kyanite-biotite zone (point 1), upper kyanite-biotite zone (point 2), and sillimanite zone (points 4, 5). Point 3 is inferred from pressure-temperature path calculation (Spear and Selverstone, 1983) using zoned garnet in sillimanite zone. Point 6 is determined for a sample of staurolite-biotite zone and is interpreted to reflect reequilibration rather than peak metamorphism. Arrow is inferred prograde and retrograde metamorphic field gradient for Juneau pelitic schists (see Himmelberg and others, 1991, for discussion). Low-grade metamorphic field gradient (long dash) is extrapolated from data of Himmelberg and others (in press). Alm, almandine; And, andalusite; Ann, annite; AS, aluminosilicate; Bt, biotite; Chl, chlorite; Cld, chloritoid; Crd, cordierite; Fe, iron; Grt, garnet; Kfs, K-feldspar; Ky, kyanite; Ms, muscovite; Prl, pyrophyllite; Qtz, quartz; Sil, sillimanite; St, staurolite.

**Table 4.** Representative analyses of chlorite from the Juneau area.

[Leaders (—), not detected]

| | Biotite zone | |
|---|---|---|
| | 79GH5A | 79GH11B |
| $SiO_2$ | 26.6 | 27.2 |
| $TiO_2$ | 0.04 | 0.10 |
| $Al_2O_3$ | 20.8 | 22.2 |
| FeO[1] | 24.6 | 17.0 |
| MnO | 0.40 | 0.10 |
| MgO | 15.1 | 9.8 |
| CaO | 0.02 | — |
| $Na_2O$ | 0.08 | 0.03 |
| $K_2O$ | 0.03 | — |
| Total | 87.67 | 86.43 |
| **Formula normalized to 14 oxygens** | | |
| Si | 2.788 | 2.767 |
| $Al^{IV}$ | 1.212 | 1.233 |
| $Al^{VI}$ | 1.358 | 1.428 |
| Ti | 0.003 | 0.008 |
| Fe | 2.156 | 1.446 |
| Mn | 0.036 | 0.009 |
| Mg | 2.359 | 3.002 |
| Ca | 0.002 | — |
| Na | 0.016 | 0.006 |
| K | 0.004 | — |
| Mg/(Mg+Fe) | 0.52 | 0.67 |

[1]Total iron calculated as FeO.

**Table 5.** Representative analyses of plagioclase from the Juneau area.

[Ky, kyanite; Bt, biotite; An, anorthite; Ab, albite; Or, orthoclase]

| | Lower Ky-Bt zone | | Sillimanite zone | | |
|---|---|---|---|---|---|
| | 79GH28A | 79GH33A | 79GH46A | 79GH52A | 79GH100B |
| $SiO_2$ | 63.2 | 62.9 | 62.2 | 62.7 | 59.0 |
| $Al_2O_3$ | 22.8 | 23.0 | 23.4 | 23.1 | 25.5 |
| CaO | 3.45 | 3.56 | 4.50 | 3.92 | 6.75 |
| $Na_2O$ | 9.62 | 9.57 | 9.03 | 9.34 | 7.71 |
| $K_2O$ | 0.12 | 0.10 | 0.16 | 0.09 | 0.30 |
| Total | 99.19 | 99.13 | 99.29 | 99.15 | 99.22 |
| **Formula normalized to 8 oxygens** | | | | | |
| Si | 2.909 | 2.898 | 2.871 | 2.891 | 2.653 |
| Al | 1.053 | 1.065 | 1.085 | 1.070 | 1.349 |
| Ca | 0.170 | 0.176 | 0.223 | 0.194 | 0.325 |
| Na | 0.859 | 0.855 | 0.807 | 0.835 | 0.672 |
| K | 0.007 | 0.006 | 0.009 | 0.005 | 0.017 |
| An | 16.4 | 16.9 | 21.4 | 18.7 | 32.1 |
| Ab | 82.9 | 82.5 | 77.7 | 80.8 | 66.3 |
| Or | 0.7 | 0.6 | 0.9 | 0.5 | 1.7 |

samples is greater than reasonable for the field interval involved and thus probably also reflects bulk rock compositional variation. The most Fe-rich biotite is greenish brown in color and occurs in a calcareous biotite-chlorite-muscovite schist in the low-grade biotite zone. The most Mg-rich biotite coexists with the most Mg-rich staurolite analyzed. Biotite is chemically unzoned, and no compositional differences exist between biotite porphyroblasts and matrix biotite in the same sample nor between biotite in contact with garnet or staurolite relative to matrix biotite. Biotite enclosed in garnet in sample 79GH52A,

**Table 6.** Representative analyses of muscovite from the Juneau area.

[St, staurolite; Bt biotite; Ky, kyanite; Ms, muscovite; Pg, paragonite; Ba, barium mica]

| | St-Bt zone | Lower Ky-Bt zone | | | | Sillimanite zone |
|---|---|---|---|---|---|---|
| | 79GH22A | 79GH25A | 79GH25C | 79GH28A | 79GH33A | 79GH52A |
| $SiO_2$ | 46.9 | 46.2 | 47.3 | 46.4 | 46.4 | 46.8 |
| $TiO_2$ | 0.43 | 0.54 | 0.51 | 0.57 | 0.76 | 1.27 |
| $Al_2O_3$ | 36.1 | 35.3 | 36.0 | 34.2 | 35.0 | 34.6 |
| FeO[1] | 0.93 | 0.81 | 0.74 | 1.27 | 1.30 | 1.28 |
| MgO | 0.59 | 0.50 | 0.51 | 1.00 | 0.87 | 0.47 |
| BaO | 2.05 | 2.77 | 2.77 | 2.48 | 1.54 | 0.27 |
| $Na_2O$ | 1.73 | 1.89 | 2.12 | 0.86 | 0.90 | 1.00 |
| $K_2O$ | 7.80 | 7.38 | 7.19 | 9.15 | 9.43 | 10.00 |
| Total | 96.53 | 95.39 | 97.14 | 95.93 | 96.20 | 95.69 |
| **Formula normalized to 11 oxygens** | | | | | | |
| Si | 3.082 | 3.086 | 3.095 | 3.104 | 3.077 | 3.013 |
| $Al^{IV}$ | 0.918 | 0.914 | 0.905 | 0.896 | 0.923 | 0.897 |
| $Al^{VI}$ | 1.879 | 1.865 | 1.871 | 1.805 | 1.820 | 1.806 |
| Ti | 0.021 | 0.027 | 0.025 | 0.029 | 0.038 | 0.064 |
| Fe | 0.051 | 0.045 | 0.040 | 0.071 | 0.072 | 0.072 |
| Mg | 0.058 | 0.050 | 0.050 | 0.100 | 0.086 | 0.046 |
| Ba | 0.053 | 0.073 | 0.071 | 0.065 | 0.040 | 0.007 |
| Na | 0.220 | 0.245 | 0.269 | 0.112 | 0.116 | 0.129 |
| K | 0.653 | 0.629 | 0.600 | 0.781 | 0.799 | 0.847 |
| Ms | 0.705 | 0.665 | 0.638 | 0.816 | 0.837 | 0.861 |
| Pg | 0.238 | 0.259 | 0.286 | 0.117 | 0.121 | 0.132 |
| Ba | 0.057 | 0.077 | 0.076 | 0.068 | 0.042 | 0.007 |

[1]Total iron calculated as FeO.

however, has a higher Mg/(Mg+Fe) ratio (0.50) than matrix biotite (0.45), even where the matrix biotite is in contact with garnet. The biotite enclosed in garnet also has a lower $TiO_2$ content (1.63 percent) than the matrix biotite (2.57 percent). $TiO_2$ content in all biotite analyzed ranges from about 1.12 to about 3.55 weight percent but not in relation to metamorphic grade as was reported by other workers (Guidotti, 1970; Fletcher and Greenwood, 1979; McLellan, 1985). Rare samples have a millimeter-scale layering with different color biotites in different layers; the biotite Mg/(Mg+Fe) ratios in adjacent layers differ by 0.05 and $TiO_2$ contents differ by more than 1 weight percent. Retention of the biotite compositional differences indicates that the scale of intergrain metamorphic diffusion was restricted to millimeters or less.

Analyzed garnets are almandine rich (table 9). Using average rim and core compositions, the garnet components reported here and in Himmelberg and others (1991) range from about 46 to 75 percent almandine, 6 to 18 percent pyrope, 4 to 25 percent grossular, and 3 to 30 percent spessartine. The Mg/(Mg+Fe) ratio is generally between 0.1 and 0.2, although two samples have values of about 0.28. Most garnets are compositionally zoned, and compositions of individual points may fall outside the ranges given above. Maximum compositional zoning for a single grain is 15 mole percent almandine, 10 mole percent pyrope, 12 mole percent grossular, and 17 mole percent spessartine. Core to rim compositional zoning profiles for garnets in the garnet zone through the kyanite-

**Table 7.** Representative analyses of staurolite from the Juneau area.

[St, staurolite; Bt, biotite; Ky, kyanite]

| | St-Bt zone | | | Lower Ky-Bt zone | | |
|---|---|---|---|---|---|---|
| | 79GH21A | 79GH22A | 79GH23B | 79GH25A | 79GH25C | 79GH35A |
| $SiO_2$ | 28.2 | 27.7 | 28.3 | 27.5 | 27.8 | 27.8 |
| $TiO_2$ | 0.44 | 0.56 | 0.25 | 0.64 | 0.59 | 0.64 |
| $Al_2O_3$ | 53.3 | 53.5 | 52.5 | 53.6 | 52.5 | 52.9 |
| FeO[1] | 10.9 | 12.7 | 9.50 | 13.8 | 13.8 | 12.8 |
| MnO | 0.17 | 0.18 | 0.48 | 0.17 | 0.22 | 0.38 |
| MgO | 1.81 | 1.79 | 2.07 | 1.90 | 1.94 | 1.79 |
| ZnO | 2.79 | 1.46 | 3.85 | 0.41 | 0.61 | 1.12 |
| Total | 97.61 | 97.89 | 96.95 | 98.02 | 97.46 | 97.43 |
| Formula normalized to 23 oxygens | | | | | | |
| Si | 3.924 | 3.853 | 3.967 | 3.821 | 3.890 | 3.884 |
| Al | 8.740 | 8.771 | 8.674 | 8.777 | 8.658 | 8.712 |
| Ti | 0.046 | 0.059 | 0.026 | 0.067 | 0.062 | 0.067 |
| Fe | 1.268 | 1.477 | 1.114 | 1.603 | 1.615 | 1.496 |
| Mn | 0.020 | 0.021 | 0.057 | 0.020 | 0.026 | 0.045 |
| Mg | 0.375 | 0.371 | 0.433 | 0.393 | 0.405 | 0.373 |
| Zn | 0.287 | 0.150 | 0.399 | 0.042 | 0.063 | 0.116 |
| Mg/(Mg+Fe) | 0.23 | 0.20 | 0.28 | 0.20 | 0.20 | 0.20 |

[1]Total iron calculated as FeO.

biotite zone are typical growth-zoning patterns (Tracy, 1982). The garnet profiles in the sillimanite zone are typical diffusion homogenized compositional patterns modified by post-growth retrograde reequilibration (Tracy, 1982). Illustrations of these patterns and a discussion of the specific details were given by Himmelberg and others (1991).

## ESTIMATION OF FLUID COMPOSITION

The $H_2O$ content of the fluid phase present during the metamorphism of the Juneau pelitic schists can be estimated from the dehydration equilibria involved in the breakdown of muscovite and staurolite and from considering the distribution of species in the C-O-H system in the presence of graphite. French (1966) and Ohmoto and Kerrick (1977) have shown that, under typical metamorphic conditions with graphite present, $H_2O$, $CO_2$, and $CH_4$ are the principal fluid species present and that because of the equilibrium

$$2C+2H_2O=CO_2+CH_4 \qquad (9)$$

pure water is not stable. The mole fraction of $H_2O$ in fluids of graphite-bearing rocks is a slowly varying function of T and P and a rapidly varying function of oxygen fugacity ($f_{O_2}$) (Ohmoto and Kerrick, 1977); if T, P, and $f_{O_2}$ are known then the mole fraction of $H_2O$ ($X_{H_2O}$) can be uniquely determined. An independent determination of $f_{O_2}$ is not available for the Juneau pelitic schists; nevertheless, the maximum possible values of $X_{H_2O}$ for the various metamorphic zones can be determined by utilizing the data of Ohmoto and Kerrick (1977) for the temperatures and pressures estimated from garnet-biotite equilibrium. Maximum $X_{H_2O}$ decreases as temperature increases because reaction 9 is favored by increasing temperature (Ohmoto and Kerrick, 1977). Using the average temperatures and pressures determined for each metamorphic zone, the maximum $X_{H_2O}$ ranges from about 0.93 for the garnet zone to about 0.90 for the upper kyanite-biotite zone. If the Juneau pelitic rocks were metamorphosed as a closed system, then the values above are probably reasonable estimates because Ohmoto and Kerrick (1977) have shown that dehydration equilibria of graphite-bearing pelites in a closed system buffer $X_{H_2O}$ to maximum possible values during metamorphism.

The equilibrium

$$\underset{\text{paragonite}}{NaAl_3Si_3O_{10}(OH)_2}+\underset{\text{quartz}}{SiO_2}=\underset{\text{albite}}{NaAlSi_3O_8}+\underset{\text{ky/sil}}{Al_2SiO_5}+H_2O \qquad (10)$$

was applied to the three samples in the lower kyanite-biotite zone. The expression for the end-member equilibrium was taken from Lang and Rice (1985), and activity-composition relations were taken from Pigage and Greenwood (1982). Muscovite solid solution was modeled in two ways in order to determine the activity of paragonite. Model 1 assumes a simple binary solution between muscovite and paragonite; model 2 considers nonideal mixing with muscovite, paragonite, K celadonite, and Na celadonite as components (Pigage and Greenwood, 1982). Using the lower kyanite-biotite zone average temperature and pressure as determined from garnet-biotite and garnet-muscovite-plagioclase-biotite equilibria, respectively, values for $X_{H_2O}$ ranging from 0.89 to 0.64 were obtained for muscovite model 1, and values ranging from 0.77 to 0.50 were obtained for muscovite model 2. The muscovite dehydration equilibrium was also applied to sillimanite-bearing samples using the end-member equilibrium expression calculated by McLellan (1985), but anomalously high values for $X_{H_2O}$ (greater than 1) were obtained.

The dehydration equilibrium

$$\underset{\text{staurolite}}{1/2Fe_4Al_{18}Si_{7.5}O_{44}(OH)_4}+\underset{\text{quartz}}{12.5/6SiO_2}=$$

$$\underset{\text{garnet}}{2/3Fe_3Al_2Si_3O_{12}}+\underset{\text{kyanite}}{23/6Al_2SiO_5}+H_2O \qquad (11)$$

is also applicable to assemblages in the lower kyanite-biotite-zone pelitic schists. The mole fraction of $H_2O$ necessary to displace the equilibrium to the average temperature and pressure of the zone was calculated using the end-member equilibrium expression determined by Lang and Rice (1985), the activity-composition model for garnet proposed by Hodges and Spear (1982) and Hodges and Royden (1984), and activity-composition models for staurolite proposed by Pigage and Greenwood (1982) and Holdaway and others (1988). Calculated values for $X_{H_2O}$ range from 0.82 to 0.63 with no significant differences in values obtained using the two different activity-composition models for staurolite.

**Table 8.** Representative analyses of biotite from the Juneau area.

[Leaders (—), not detected. Gt, garnet; St, staurolite; Bt, biotite; Ky, kyanite]

| | Gt zone | St-Bt zone | LowerKy-Bt zone | | | | | | Sillimanite zone | | |
|---|---|---|---|---|---|---|---|---|---|---|---|
| | 79GH11B | 79GH22A | 79GH23A | 79GH23B | 79GH25A | 79GH25C | 79GH25C | 79GH33A | 79GH46A | 79GH52A | 79GH100B |
| $SiO_2$ | 38.6 | 38.2 | 38.8 | 38.8 | 37.8 | 37.0 | 36.6 | 36.6 | 36.5 | 35.9 | 37.3 |
| $TiO_2$ | 1.81 | 1.72 | 1.73 | 1.12 | 1.83 | 1.74 | 2.83 | 2.50 | 2.68 | 2.57 | 1.38 |
| $Al_2O_3$ | 17.5 | 19.6 | 19.4 | 19.8 | 19.3 | 19.6 | 19.3 | 19.8 | 19.8 | 19.9 | 20.4 |
| FeO[1] | 14.2 | 17.2 | 11.7 | 11.6 | 16.7 | 17.0 | 16.0 | 17.3 | 18.4 | 19.5 | 14.3 |
| MnO | --- | 0.06 | 0.17 | 0.15 | 0.07 | 0.06 | 0.35 | 0.24 | 0.10 | 0.13 | 0.10 |
| MgO | 13.8 | 11.4 | 15.0 | 15.2 | 11.4 | 11.2 | 11.2 | 10.6 | 9.35 | 8.90 | 13.4 |
| CaO | 0.04 | --- | --- | --- | --- | --- | --- | --- | --- | --- | 0.07 |
| $Na_2O$ | 0.23 | 0.32 | 0.34 | 0.37 | 0.44 | 0.40 | 0.26 | 0.32 | 0.40 | 0.35 | 0.26 |
| $K_2O$ | 8.42 | 8.63 | 8.63 | 8.29 | 8.27 | 8.56 | 8.91 | 9.03 | 8.82 | 9.30 | 9.34 |
| Total | 94.60 | 97.13 | 95.77 | 95.33 | 95.81 | 95.56 | 95.45 | 96.39 | 96.05 | 96.55 | 96.55 |
| Formula normalized to 11 oxygens | | | | | | | | | | | |
| Si | 2.849 | 2.787 | 2.797 | 2.799 | 2.787 | 2.752 | 2.723 | 2.713 | 2.725 | 2.689 | 2.716 |
| $Al^{IV}$ | 1.151 | 1.213 | 1.203 | 1.201 | 1.213 | 1.248 | 1.277 | 1.287 | 1.275 | 1.311 | 1.284 |
| $Al^{VI}$ | 0.374 | 0.471 | 0.444 | 0.487 | 0.468 | 0.463 | 0.416 | 0.439 | 0.463 | 0.448 | 0.467 |
| Ti | 0.100 | 0.094 | 0.094 | 0.061 | 0.101 | 0.097 | 0.158 | 0.139 | 0.150 | 0.145 | 0.076 |
| Fe | 0.878 | 1.047 | 0.705 | 0.701 | 1.029 | 1.054 | 0.994 | 1.072 | 1.149 | 1.221 | 0.871 |
| Mn | --- | 0.004 | 0.010 | 0.009 | 0.004 | 0.004 | 0.022 | 0.015 | 0.006 | 0.008 | 0.006 |
| Mg | 1.520 | 1.236 | 1.611 | 1.632 | 1.248 | 1.243 | 1.241 | 1.170 | 1.039 | 0.994 | 1.455 |
| Ca | 0.003 | --- | --- | --- | --- | --- | --- | --- | --- | --- | 0.005 |
| Na | 0.033 | 0.046 | 0.048 | 0.051 | 0.063 | 0.058 | 0.037 | 0.045 | 0.058 | 0.051 | 0.037 |
| K | 0.793 | 0.802 | 0.793 | 0.763 | 0.779 | 0.811 | 0.845 | 0.853 | 0.839 | 0.889 | 0.868 |
| Mg/(Mg+Fe) | 0.63 | 0.54 | 0.70 | 0.70 | 0.55 | 0.54 | 0.56 | 0.52 | 0.47 | 0.45 | 0.62 |

[1]Total iron calculated as FeO.

The values obtained for mole fraction of $H_2O$ from the muscovite and staurolite equilibria are generally consistent but less than the values indicated by the C-O-H equilibria. Values of $X_{H_2O}$ calculated from the muscovite and staurolite equilibria, however, are extremely sensitive to temperature, and considering the uncertainty in the temperature determinations, the mole fraction of $H_2O$ is probably better constrained by the distribution of species in the C-O-H system for graphitic schists.

## SUMMARY

The western metamorphic belt underwent a complex history of deformation, metamorphism, and plutonism that ranges in age from about 120 Ma to about 50 Ma (Crawford and others, 1987; Brew and others, 1989). The protoliths for the western metamorphic belt were mainly the heterogeneous Alexander terrane rocks of Permian and Triassic age and the flysch and volcanic rocks of the Gravina overlap assemblage (Berg and others, 1972) of Late Jurassic through early Late Cretaceous age. In the Juneau area, the metamorphic rocks consist dominantly of intermixed pelitic and semipelitic metasedimentary rocks, and mafic metavolcanic and intrusive rocks. Impure calcareous metasedimentary rocks, quartzite, and quartz diorite and granodioritic orthogneiss are also present.

Most of the schists and gneisses in the Juneau area are products of the M5 metamorphic event of Brew and others (1989), which they interpreted to have occurred between about 70 Ma and 65 Ma. The mineral isograds, systematic changes in mineral assemblages, and structural relations indicate an inverted metamorphic gradient along the easternmost part of the belt, where the metamorphic grade goes abruptly from greenschist facies to kyanite- and sillimanite-bearing amphibolite facies in less than 5 km across strike. The westernmost part of the belt consists of metabasites metamorphosed to pumpellyite-actinolite facies during the M1 metamorphic event. The major schistosity, $S_1$, is subparallel to compositional layering and is interpreted to have formed during the regional D1 deformational event. The D3 deformation event, which was synchronous with M5 metamorphism, folded the $S_1$ schistosity about gently plunging northwest trending axes. $F_3$ axial planes are generally steep and development of an $S_3$ axial plane foliation is variable. On the limbs of folds $S_1$ and $S_3$ foliation are subparallel and not readily distinguished. No large-scale structures or minor folds associated with the D1 deformation event have been clearly identified, although there is some suggestion that the D1 and D3 deformation events may have been nearly coaxial. The isograd surfaces strike northwest and dip to the northeast, parallel or subparallel to the dominant metamorphic $S_1$-$S_3$ foliation.

Pelitic mineral assemblages produced during the M5 metamorphic event define six metamorphic zones—biotite, garnet, staurolite-biotite, lower kyanite-biotite, upper kyanite-biotite, and sillimanite. Isograds separating the zones are in general agreement with discontinuous reactions in the ideal KMFASH system. Peak temperatures of metamorphism increase progressively from about 530°C for the garnet zone to about 705°C for the upper kyanite-biotite zone. Silicate geobarometry suggests that the thermal peak metamorphism occurred under pressures

**Table 9.** Representative analyses of garnet from the Juneau area.

[Leaders (—), not detected; n.d., not determined. C, average core composition; NR, average rim or near-rim composition; where no symbol is given there is no distinction between core and rim. St, staurolite; Bt, biotite; Ky, kyanite; Prp, pyrope; Grs, grossularite; Sps, spessartine; Alm, almandine]

| | St-Bt zone | | Lower Ky-Bt zone | | | | | | | Sillimanite zone | | | | | |
|---|---|---|---|---|---|---|---|---|---|---|---|---|---|---|---|
| | 79GH22A | 79GH22A | 79GH23A | 79GH23A | 79GH25A | 79GH25C | 79GH25C | 79GH28A | 79GH33A | 79GH46A | 79GH46A | 79GH52A | 79GH52A | 79GH100B | 79GH100B |
| | C | NR | C | NR | C | C | NR | | | C | NR | C | NR | C | NR |
| $SiO_2$ | 37.1 | 37.2 | 38.1 | 38.0 | 37.5 | 37.4 | 37.2 | 38.2 | 37.2 | 37.5 | 38.0 | 38.1 | 37.9 | 38.7 | 38.0 |
| $TiO_2$ | 0.19 | — — — | 0.14 | 0.55 | n.d. | n.d. | n.d. | 0.04 | 0.08 | 0.01 | 0.01 | 0.03 | 0.01 | 0.02 | — — — |
| $Al_2O_3$ | 21.8 | 21.9 | 21.7 | 22.0 | 22.5 | 22.6 | 22.4 | 22.2 | 22.0 | 22.0 | 22.2 | 22.0 | 22.1 | 22.3 | 22.2 |
| $FeO^1$ | 29.0 | 33.2 | 21.2 | 24.3 | 32.4 | 31.9 | 32.1 | 25.7 | 28.6 | 31.7 | 33.1 | 32.5 | 32.0 | 27.9 | 29.3 |
| MnO | 6.74 | 2.08 | 13.0 | 8.72 | 2.60 | 3.56 | 3.42 | 8.82 | 6.34 | 2.48 | 1.38 | 2.08 | 4.57 | 1.94 | 4.05 |
| MgO | 2.41 | 3.09 | 3.26 | 4.61 | 3.40 | 3.25 | 3.29 | 3.39 | 3.24 | 2.54 | 4.11 | 4.23 | 3.33 | 7.11 | 5.00 |
| CaO | 3.44 | 3.13 | 4.22 | 3.08 | 2.84 | 2.79 | 2.76 | 3.03 | 2.41 | 4.04 | 1.88 | 1.74 | 0.96 | 2.25 | 1.69 |
| Total | 100.68 | 100.60 | 101.62 | 101.26 | 101.24 | 101.50 | 101.12 | 101.38 | 99.87 | 100.26 | 100.68 | 100.71 | 100.88 | 100.24 | 100.30 |
| | Formula normalized to 12 oxygens | | | | | | | | | | | | | | |
| Si | 2.963 | 2.965 | 2.990 | 2.982 | 2.957 | 2.947 | 2.946 | 2.997 | 2.976 | 2.989 | 2.997 | 3.004 | 2.999 | 3.001 | 2.990 |
| $Al^{IV}$ | 0.037 | 0.035 | 0.010 | 0.018 | 0.043 | 0.053 | 0.054 | 0.003 | 0.024 | 0.011 | 0.003 | 0.000 | 0.001 | 0.000 | 0.010 |
| $Al^{VI}$ | 2.015 | 2.019 | 1.998 | 2.018 | 2.048 | 2.046 | 2.032 | 2.050 | 2.048 | 2.053 | 2.058 | 2.041 | 2.063 | 2.037 | 2.051 |
| Ti | 0.011 | — — — | 0.008 | 0.004 | n.d. | n.d. | n.d. | 0.002 | 0.005 | 0.001 | 0.001 | 0.002 | 0.001 | 0.001 | — — — |
| Fe | 1.937 | 2.215 | 1.392 | 1.596 | 2.137 | 2.102 | 2.126 | 1.685 | 1.909 | 2.111 | 2.180 | 2.144 | 2.123 | 1.806 | 1.930 |
| Mn | 0.456 | 0.140 | 0.864 | 0.580 | 0.174 | 0.238 | 0.229 | 0.586 | 0.429 | 0.167 | 0.092 | 0.139 | 0.307 | 0.127 | 0.270 |
| Mg | 0.287 | 0.367 | 0.382 | 0.540 | 0.400 | 0.382 | 0.388 | 0.396 | 0.386 | 0.302 | 0.483 | 0.496 | 0.393 | 0.821 | 0.587 |
| Ca | 0.294 | 0.267 | 0.355 | 0.259 | 0.240 | 0.236 | 0.234 | 0.255 | 0.206 | 0.345 | 0.159 | 0.147 | 0.081 | 0.186 | 0.142 |
| Prp | 9.6 | 12.3 | 12.7 | 18.1 | 13.5 | 12.9 | 13.0 | 13.6 | 13.2 | 10.3 | 16.6 | 17.0 | 13.5 | 27.9 | 20.0 |
| Grs | 9.9 | 8.9 | 11.9 | 8.8 | 8.1 | 8.0 | 7.9 | 8.7 | 7.0 | 11.8 | 5.5 | 5.0 | 2.8 | 6.3 | 4.9 |
| Sps | 15.3 | 4.7 | 28.9 | 19.4 | 5.9 | 8.0 | 7.7 | 20.0 | 14.6 | 5.7 | 3.2 | 4.7 | 10.6 | 4.3 | 9.2 |
| Alm | 65.1 | 74.1 | 46.5 | 53.6 | 72.4 | 71.1 | 71.4 | 57.7 | 65.1 | 72.2 | 74.8 | 73.3 | 73.1 | 61.4 | 65.9 |

[1]Total iron calculated as FeO.

of 9 to 11 kbar. The sequence of reactions and the calculated pressure and temperature for the individual metamorphic zones are consistent with the petrogenetic grid of Spear and Cheney (1989). Changes in Mg/(Mg+Fe) ratio of biotite and staurolite with increasing metamorphic grade in three- and four-phase assemblages appropriate to reactions in the KMFASH system are generally consistent with the changes predicted by Thompson (1976), although exceptions do exist. Changes in garnet composition in the same assemblages are complicated, owing to complex zoning patterns and retrograde equilibration of some rim compositions. On the basis of the distribution of species in the C-O-H system for graphitic schists, the mole fraction of $H_2O$ during metamorphism probably ranged from about 0.93 for the garnet zone to about 0.90 for the kyanite-biotite zone.

## REFERENCES CITED


Albee, A.L., and Ray, L., 1970, Correction factors for electron probe microanalysis of silicates, oxides, carbonates, phosphates, and sulfates: Analytical Chemistry, v. 42, p. 1408–1414.

Bauer, R.L., Himmelberg, G.R., Brew, D.A., and Ford, A.B., 1988, Relative timing of porphyroblast growth, foliation development, and ductile shear in pelitic metamorphic rocks from the Juneau area, southeastern Alaska, *in* Galloway, J.P. and Hamilton, T.P., eds., Geological studies in Alaska by the U.S. Geological Survey during 1987: U.S. Geological Survey Circular 1016, p. 138–142.

Bell, T.H., and Rubenach, M.J., 1983, Sequential porphyroblast growth and crenulation cleavage development during progressive deformation: Tectonophysics, v. 92, p. 171–194.

Bence, A.E., and Albee, A.L., 1968, Empirical correction factors for the electron microanalysis of silicates and oxides: Journal of Geology, v. 76, p. 382–403.

Berg, H.C., Jones, D.L., and Richter, D.H., 1972, Gravina-Nutzotin belt—Tectonic significance of an upper Mesozoic sedimentary and volcanic sequence in southern and southeastern Alaska, *in* Geological Survey Research, 1972: U.S. Geological Survey Professional Paper 800 D, p. D1–D24.

Brew, D.A., 1988, Late Mesozoic and Cenozoic igneous rocks of southeastern Alaska—A synopsis: U.S. Geological Survey Open-File Report 88-405, 29 p.

Brew, D.A., and Ford, A.B., 1977, Preliminary geologic and metamorphic-isograd map of the Juneau B-1 quadrangle, Alaska: U.S. Geological Survey Miscellaneous Field Studies Map MF-846, scale 1:31,680.

———1978, Megalineament in southeastern Alaska marks southwest edge of Coast Range batholithic complex: Canadian Journal of Earth Sciences, v. 15, p. 1763–1762.

———1983, Comment on "Tectonic accretion and the origin of the two major metamorphic and plutonic welts in the Canadian Cordillera": Geology, v. 11, p. 427–428.

———1984, Tectonostratigraphic terranes in the Coast plutonic-metamorphic complex, southeastern Alaska, *in* Barsch-Winkler, S., and Reed ,K., eds., The United States Geological Survey in Alaska: Miscellaneous geologic research 1982: U.S. Geological Survey Circular 939, p. 90–93.

Brew, D.A., Ford, A.B., and Himmelberg, G.R., 1989, Evolution of the western part of the Coast plutonic-metamorphic complex, southeastern Alaska, U.S.A.: A summary, *in* Daly, S.R., Cliff, R.A., and Yardley, B.W., eds., Evolution of metamorphic belts: Geological Society Special Publication 43, p. 447–452.

Brew, D.A., Himmelberg, G.R., Loney, R.A., and Ford, A.B., 1992, Distribution and characteristics of metamorphic belts in the south-eastern Alaska part of the North America Cordillera: Journal of Metamorphic Geology, v. 10, p. 465–482.

Brew, D.A., and Morrell, R.P., 1983, Intrusive rocks and plutonic belts of southeastern Alaska, U.S.A, *in* Roddick, J.A., ed., Circum-pacific plutonic terranes: Geological Society of America Memoir 159, p. 171–193.

Brew, D.A., Ovenshine, A.T., Karl, S.M., and Hunt, S.J., 1984, Preliminary reconnaissance geologic map of the Petersburg and parts of the Port Alexander and Sumdum 1:250,000 quadrangles, southeastern Alaska: U.S. Geological Survey Open-File Report 84-405, 2 sheets, 43 p. pamphlet.

Carmichael, D.M., 1970, Intersecting isograds in the Whetstone Lake area, Ontario. Journal of Petrology, 11, 147–181.

Crawford, M.L., Hollister, L.S., and Woodsworth, G.J., 1987, Crustal deformation and regional metamorphism across a terrane boundary, Coast Plutonic Complex, British Columbia: Tectonics, v. 6, p. 343–361.

Donelick, R.A., 1986, Mesozoic-Cenozoic thermal evolution of the Atlin terrane, Whitehorse Trough, and Coast Plutonic Complex from Atlin, British Columbia to Haines, Alaska as revealed by fission track-geothermometry techniques: Troy, New York, Rensselaer Polytechnic Institute, M.S. thesis, 167 p.

Dymek, R.F., 1983, Titanium, aluminum, and interlayer cation substitutions in biotite from high-grade gneisses, West Greenland: American Mineralogist, v. 68, p. 880–899.

Fletcher, C.J.N., and Greenwood, H.J., 1979, Metamorphism and structure of the Penfold Creek area, near Quesnel Lake, British Columbia: Journal of Petrology, v. 20, p. 743-794.

Forbes, R.B., 1959, The geology and petrology of the Juneau Ice Field area, southeastern Alaska: Seattle, University of Washington, Ph.D. dissertation, 261 p.

Forbes, R.B., and Engels, J.C., 1970, $K^{40}/Ar^{40}$ age relations of the Coast Range batholith and related rocks of the Juneau ice field area, Alaska: Geological Society of America Bulletin, v. 81, p. 579–584.

Ford, A.B., and Brew, D.A., 1973, Preliminary geologic and metamorphic-isograd map of the Juneau B-2 quadrangle, Alaska: U.S. Geological Survey Miscellaneous Field Studies Map MF-527, scale 1:31,680.

———1977a, Preliminary geologic and metamorphic-isograd map of the Juneau A-1 and A-2 quadrangles, Alaska: U.S. Geological Survey Miscellaneous Field Map MF-847., scale 1:31,680.

———1977b, Truncation of regional metamorphic zonation pattern of the Juneau , Alaska, area by the Coast Range batholith, *in* Blean, K.M., ed., The United States Geological Survey in Alaska: Accomplishments during 1976: U.S. Geological Circular 751-B, p. B85–B87.

French, B.M., 1966, Some geological implications of equilibrium between graphite and a C-H-O gas phase at high temperatures and pressures: Reviews of Geophysics, v. 4, p. 223–253.

Gehrels, G.E., Brew, D.A., and Saleeby, J.B., 1984, Progress report on U/PB (zircon) geochronologic studies in the Coast plutonic-metamorphic complex east of Juneau, southeastern Alaska, *in* Reed, K.M. and Bartsch-Winkler, S., ed., The United States Geological Survey in Alaska: Accomplishments during 1982: U.S. Geological Survey Circular 939, p. 100–102.

Gehrels, G.E., McClelland, W.C., Samson, S.D., Patchett, P.J., and Brew, D.A., 1991, U-Pb geochronology of Late Cretaceous and early Tertiary plutons in the northern Coast Mountains batholith: Canadian Journal Earth Sciences, v. 28, p. 899–911.

Geological Society of America, 1984, Decade of North American Geology Geologic Time Scale: Geological Society of America Map and Chart Series, MC-50.

Guidotti, C.V., 1970, The mineralogy and petrology of the transition from the lower to upper sillimanite zone, in the Oquossoc area, Maine: Journal of Petrology, v. 11, p. 277–336.

———1974, Transition from staurolite to sillimanite zone, Rangely quadrangle, Maine: Geological Society of America Bulletin, v. 85, p. 475–490.

———1984, Micas in metamorphic rocks: Mineralogical Society of America Reviews in Mineralogy, v. 13, p. 357–467.

Himmelberg, G.R., Brew, D.A., and Ford, A.B., 1991, Development of inverted metamorphic isograds in the western metamorphic belt, Juneau, Alaska: Journal of Metamorphic Geology, v. 9, p. 165–180.

———in press, Low-grade metamorphism of the Douglas Island Volcanics: Earliest recognized metamorphic event in the western metamorphic belt near Juneau Alaska: Geological Society of America Special Paper.

Himmelberg, G.R., Ford, A.B., and Brew, D.A., 1984a, Progressive metamorphism of pelitic rocks in the Juneau area, southeastern Alaska, *in* Coonrad, W.L., and Elliot, R.L., eds., The United States Geological Survey in Alaska—Accomplishments during 1981: U.S. Geological Survey Circular, 868, p. 131–134.

———1984b, Reaction isograds in pelitic rocks of the Coast Plutonic-Metamorphic Complex near Juneau, *in* Reed, K.M., and Bartsch-Winkler, S., eds., The United States Geological Survey in Alaska—Accomplishments during 1982: U.S. Geological Survey Circular 939, p. 105–108.

Hodges, K.V., and Royden, L., 1984, Geologic thermobarometry of retrograded metamorphic rocks: an indication of the uplift trajectory of a portion of the northern Scandinavian Caledonides: Journal of Geophysical Research, v. 89, p. 7077–7090.

Hodges, K.V., and Spear, F.S., 1982, Geothermometry, geobarometry, and the $Al_2SiO_5$ triple point at Mt. Moosilauke, New Hampshire: American Mineralogist, v. 67, p. 1118–1184.

Holdaway, M.J., Dutrow, B.L., and Hinton, R.W., 1988, Devonian and Carboniferous metamorphism in west-central Maine: The muscovite-almandine geobarometer and the staurolite problem revisited: American Mineralogist, v. 73, p. 20–47.

Holdaway, M.J., Guidotti, C.V., Novak, J.M., and Henry, W.E., 1982, Polymetamorphism in medium- to high-grade pelitic metamorphic rocks, west-central Maine: Geological Society of America Bulletin, v. 93, p. 572–584.

Hooper, R.J., Brew, D.A., Himmelberg, G.R., Stowell, H.H., Bauer, R.L., and Ford, A.B., 1990, The nature and signifi-

cance of post-thermal-peak shear zones west of the great tonalite sill near Juneau, Alaska, *in* Dover, J.H. and Galloway, J.P., eds., Geologic Studies in Alaska by the U.S. Geological Survey, 1989: U.S. Geological Survey Bulletin 1946, p. 88–94.

Klaper, E.M., and Bucher-Nurminen, K., 1987, Alpine metamorphism of pelitic schists in the Nufenen Pass area, Lepontine Alps: Journal of Metamorphic Geology, v. 5, p. 175–194.

Lang, H.M., and Rice, J.M., 1985, Geothermometry, geobarometry, and T-X(Fe-Mg) relations in metapelites, Snow Peak, northern Idaho: Journal of Petrology, v. 26, p. 889–924.

McClelland, W.C., Anovitz, L.M., and Gehrels, G.E., 1991, Thermobarometric constraints on the structural evolution of the Coast Mountains batholith, central southeastern Alaska: Canadian Journal of Earth Sciences, v. 28, p. 912–928.

McLellan, E., 1985, Metamorphic reactions in the kyanite and sillimanite zones of the Barrovian type area: Journal of Petrology, v. 26, p. 789–818.

Monger, J.W.H., Price, R.A., and Tempelman-Kluit, D.J., 1982, Tectonic accretion and the origin of the two major metamorphic and plutonic welts in the Canadian Cordillera: Geology, v. 10, p. 70–75.

Novak, J.M., and Holdaway, M.J., 1981, Metamorphic petrology, mineral equilibria, and polymetamorphism in the Augusta quadrangle, southcentral Maine: American Mineralogist, v. 66, p. 51–69.

Ohmoto, H., and Kerrick, D.M., 1977, Devolatiliztion equilibria in graphitic systems: American Journal of Science: v. 277, p. 1013–1044.

Pigage, L.C., and Greenwood, H.J., 1982, Internally consistent estimates of pressure and temperature—The staurolite problem: American Journal of Science, v. 282, p. 943–969.

Spear, F.S., and Cheney, J.T., 1989, A petrogenetic grid for pelitic schists in the system $SiO_2$-$Al_2O_3$-FeO-MgO-$K_2O$-$H_2O$: Contributions to Mineralogy and Petrology, v. 101, p. 149–164.

Spear, F.S., and Selverstone, J.E., 1983, Quantitative P-T paths from zoned minerals: Theory and tectonic applications: Contributions to Mineralogy and Petrology, v.83, p. 348–357.

Stowell, H., 1989, Silicate and sulfide thermobarometry of low- to medium-grade metamorphic rocks from Holkham Bay, south-east Alaska: Journal of Metamorphic Geology, v. 7, p. 343–358.

Thompson, A.B., 1976, Mineral reactions in pelitic rocks: I. Prediction of P-T-X (Fe-Mg) phase relations: American Journal of Science, v. 276, p. 401–425.

Thompson, J.B., 1957, The graphical analysis of mineral assemblages in pelitic schists: American Mineralogist, v. 42, p. 842–858.

Tracy, R.J., 1982, Compositional zoning and inclusions in metamorphic minerals, *in* Ferry, J.M., ed., Characterization of Metamorphism through Mineral Equilibria: Reviews in Mineralogy, v. 10, p. 355–393.

Wood, D.J., Stowell, H.H., and Onstott, T.C., 1987, Uplift and cooling rates from thermochronology ($^{40}Ar/^{39}Ar$) of the Coast plutonic complex sill, SE Alaska: Geological Society America Abstracts with Programs, v. 19, p. 896.

Zen, E-An, 1981, Metamorphic mineral assemblages of slightly calcic pelitic rocks in and around the Taconic allochthon, southwestern Massachusetts and adjacent Connecticut and New York: U.S. Geological Survey, Professional Paper 1113, 128 p.

———1988, Tectonic significance of high-pressure plutonic rocks in the western Cordillera of North America, *in* Ernst, W.G., ed., Metamorphism and crustal evolution of the western United States (Rubey volume): Englewood Cliffs, N.J., Prentice-Hall, p. 41–67.

* U.S. GOVERNMENT PRINTING OFFICE: 1994-583-048/80016